HHS Public Access

Author manuscript

Cell Rep. Author manuscript; available in PMC 2024 September 22.

Published in final edited form as:

Cell Rep. 2024 April 23; 43(4): 114089. doi:10.1016/j.celrep.2024.114089.

NKp44/HLA-DP-dependent regulation of CD8 effector T cells by NK cells

Benedetta Padoan[1], **Christian Casar**[2], **Jenny Krause**[3,4], **Christoph Schultheiss**[5,6], **Martin E. Baumdick**[1,7], **Annika Niehrs**[1], **Britta F. Zecher**[1,3], **Maria Pujantell**[1], **Yuko Yuki**[8,9], **Maureen Martin**[8,9], **Ester B.M. Remmerswaal**[10], **Tamara Dekker**[10], **Nelly D. van der Bom-Baylon**[10], **Janelle A. Noble**[11], **Mary Carrington**[8,9,12], **Frederike J. Bemelman**[13], **Rene A.W. van Lier**[14], **Mascha Binder**[5,6], **Nicola Gagliani**[3,15,16], **Madeleine J. Bunders**[1,7,16,17], **Marcus Altfeld**[1,16,17,18,*]

[1]Research Department Virus Immunology, Leibniz Institute of Virology, 20251 Hamburg, Germany

[2]Bioinformatics Core, University Medical Center Hamburg-Eppendorf, 20246 Hamburg, Germany

[3]I. Department of Medicine, University Medical Center Hamburg-Eppendorf, 20246 Hamburg, Germany

[4]Center for Immunology, University of Minnesota, Minneapolis, MN, USA

[5]Division of Medical Oncology, University Hospital Basel, 4031 Basel, Switzerland

[6]Laboratory of Translational Immuno-Oncology, Department of Biomedicine, University and University Hospital Basel, 4031 Basel, Switzerland

[7]III. Department of Medicine, University Medical Center Hamburg-Eppendorf, 20246 Hamburg, Germany

[8]Basic Science Program, Frederick National Laboratory for Cancer Research, National Cancer Institute, Frederick, MD 21702, USA

[9]Laboratory of Integrative Cancer Immunology, Center for Cancer Research, National Cancer Institute, Bethesda, MD 20892, USA

[10]Department of Experimental Immunology, Amsterdam Infection and Immunity Institute, Amsterdam UMC, University of Amsterdam, Amsterdam, the Netherlands

[11]Department of Pediatrics UCSF, Children's Hospital Oakland Research Institute, Oakland, CA 94609, USA

[12]Ragon Institute of MGH, MIT and Harvard, Cambridge, MA 02139, USA

[*]Correspondence: marcus.altfeld@leibniz-liv.de.

AUTHOR CONTRIBUTIONS

Conceptualization, B.P., M.J.B., and M.A.; data curation, B.P., C.C., C.S., and Y.Y.; formal analysis, B.P., C.C., and C.S.; funding acquisition, M.A. and M.J.B.; investigation, B.P., C.C., J.K., C.S., M.E.B., A.N., B.F.Z., M.P., Y.Y., M.M., E.B.M.R., T.D., N.D.v.d.B.-B., J.A.N., M.C., F.J.B., R.A.W.v.L., M.B., and N.G.; writing – original draft, B.P. and M.A.

DECLARATION OF INTERESTS

The authors declare no competing interests.

SUPPLEMENTAL INFORMATION

Supplemental information can be found online at https://doi.org/10.1016/j.celrep.2024.114089.

[13]Renal Transplant Unit, Division of Internal Medicine, Academic Medical Centre, Amsterdam UMC, University of Amsterdam, Amsterdam, the Netherlands

[14]University Medical Center Utrecht, Utrecht, the Netherlands

[15]Department of General, Visceral and Thoracic Surgery, University Medical Center Hamburg-Eppendorf, 20246 Hamburg, Germany

[16]Hamburg Center for Translational Immunology (HCTI), Hamburg, Germany

[17]These authors contributed equally

[18]Lead contact

SUMMARY

Although natural killer (NK) cells are recognized for their modulation of immune responses, the mechanisms by which human NK cells mediate immune regulation are unclear. Here, we report that expression of human leukocyte antigen (HLA)-DP, a ligand for the activating NK cell receptor NKp44, is significantly upregulated on $CD8^+$ effector T cells, in particular in human cytomegalovirus $(HCMV)^+$ individuals. HLA-DP^+ $CD8^+$ T cells expressing NKp44-binding HLA-DP antigens activate $NKp44^+$ NK cells, while HLA-DP^+ $CD8^+$ T cells not expressing NKp44-binding HLA-DP antigens do not. In line with this, frequencies of HLA-DP^+ $CD8^+$ T cells are increased in individuals not encoding for NKp44-binding HLA-DP haplotypes, and contain hyper-expanded $CD8^+$ T cell clones, compared to individuals expressing NKp44-binding HLA-DP molecules. These findings identify a molecular interaction facilitating the HLA-DP haplotype-specific editing of HLA-DP^+ $CD8^+$ T cell effector populations by $NKp44^+$ NK cells and preventing the generation of hyper-expanded T cell clones, which have been suggested to have increased potential for autoimmunity.

In brief

Padoan et al. show that HLA-DP expression on $CD8^+$ T cells is upregulated upon HCMV infection, in particular on effector $CD8^+$ T cells. $NKp44^+$ NK cells can regulate HLA-DP^+ $CD8^+$ T cells in individuals expressing NKp44-binding HLA-DP haplotypes, with consequences for $CD8^+$ T cell clonality.

Graphical Abstract

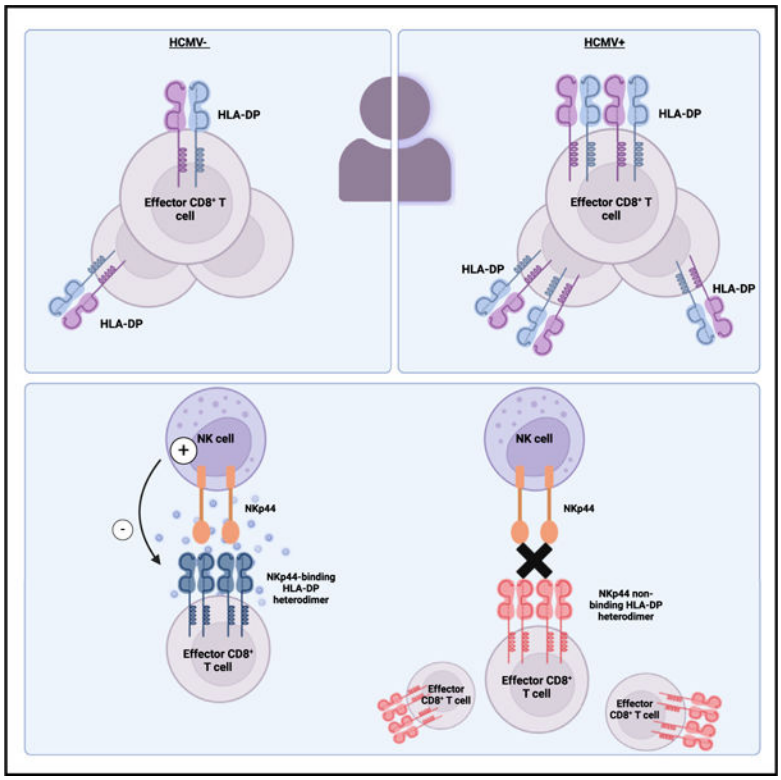

INTRODUCTION

Natural killer (NK) cells are specialized effector lymphocytes of the innate immune system that are traditionally characterized by the ability to kill virus-infected and transformed cells.[1–3] More recently, NK cells have also been implicated in the regulation of adaptive immunity. In viral infections, murine NK cells act as rheostats of adaptive immune responses by killing $CD4^+$ T cells and consequently influencing $CD8^+$ T cell responses[4,5] or by directly eliminating activated $CD8^+$ T cells.[6] NK cells can also reduce T cell responses in mice through functional restriction of antigen-presenting cells (APCs),[7] reducing immunopathology. Furthermore, stronger vaccine-induced B cell and antibody responses were observed in mice when NK cells were depleted at the time of vaccination.[8,9] While these studies demonstrate that NK cells can reduce adaptive immune responses to viral infections and vaccines, the absence of NK cells also enhanced the risk for the development of autoimmune diseases.[10] NK cell-dependent elimination of activated T cells has been shown to restrict the expansion of autoreactive T cells in a model of autoimmune encephalomyelitis,[11] and induction of tissue-resident NK cells in the salivary gland[12] reduced autoimmunity associated with murine cytomegalovirus infection.[13]

Given the emerging role of NK cells in regulating T cell immunity,[14–16] identifying the receptor-ligand interactions involved in this immunoregulatory process is of fundamental importance. Several NK cell receptors have been implicated in the regulation of T cell function. Studies in mouse models have shown that the inhibitory NK cell receptors 2B4 and NKG2A facilitate the development and expansion of memory T cells.[11,17] In

contrast, the expression of the tumor necrosis factor (TNF)-related apoptosis-inducing ligand and/or the engagement of the activating NKG2D receptor on NK cells resulted in the killing of activated T cells.[13,18] Type I interferons were shown to protect antiviral murine $CD8^+$ T cells from NK cell-mediated lysis by downregulating the expression of ligands for the activating NK cell receptor NCR1.[19,20] Studies in hepatitis B virus (HBV)-infected individuals have furthermore demonstrated that differentiated antiviral $CD8^+$ T cells upregulatePD1 expression and are restrictedby PD-L1-expressing NK cells.[21,22] In line with these observations, the presence of inhibitory killer cell immunoglobulin-like receptors (iKIRs) expressed on NK cells has been associated with an extended lifespan of human $CD8^+$ T cells *in vivo*[23] and better $CD8^+$ T cell-mediated control of HIV-1, HCV, and human T-lymphotropic virus 1 infection in humans.[24] iKIRs bind to human leukocyte antigen class I (HLA-I) molecules,[3] implicating HLA-I diversity in determining the strength of NK cell-mediated regulation of T cell immunity, and combined KIR/HLA-I genotypes have been associated with differential disease outcomes in several viral infections.[25–28]

Another family of highly polymorphic cell surface proteins are HLA-II antigens. HLA-II antigens (DR, DQ, and DP) are heterodimeric proteins, comprised of an α and a β chain encoded by an A and a B gene, respectively. HLA-DP is a heterodimer that includes the product of the *HLA-DPA1* and the *HLA-DPB1* genes, and genetic variations in HLA-II molecules have been associated with the outcome of autoimmune diseases.[29–33] Recently, it was shown that some HLA-DP molecules can serve as ligands for the activating natural cytotoxicity receptor (NCR) NKp44 (e.g., NKp44-binding HLA-DP antigens), while others do not bind NKp44 (e.g., NKp44 non-binding HLA-DP antigens),[34] providing a model to investigate the impact of NKp44/HLA-DP interactions on the regulation of $CD8^+$ T cells. Here, we show that effector $CD8^+$ T cells express HLA-DP, in particular in human cytomegalovirus $(HCMV)^+$ individuals, and that $NKp44^+$ NK cells are activated by HLA-DP^+ $CD8^+$ T cell populations in an HLA-DP haplotype-dependent process. In line with HLA-DP haplotype-dependent regulation of $CD8^+$ T cell populations by $NKp44^+$ NK cells, frequencies of HLA-DP^+ $CD8^+$ T cells were increased in individuals encoding for NKp44 non-binding HLA-DP antigens and contained hyper-expanded $CD8^+$ T cell clones compared to individuals expressing NKp44-binding HLA-DP molecules.

RESULTS

HLA-DP, but not other HLA-II molecules, are significantly expressed by $CD8^+$ T cells

HLA-II molecules are typically expressed on APCs, but expression can be upregulated on other parenchymal and immune cells upon activation.[35] However, less is known regarding HLA-II expression on resting T cells. To investigate HLA-II expression on T cells, we analyzed freshly isolated human peripheral blood cells using flow cytometry. While $CD3^+$ T cells expressed low levels of HLA-DQ and HLA-DR, HLA-DP surface expression levels were significantly higher, with a median of 26.8% of $CD3^+$ T cells expressing HLA-DP. The frequencies of T cells expressing HLA-DP were particularly high within $CD3^+CD8^+$ T cells compared to $CD3^+CD4^+$ T cells, with medians of 36.2% and 8.3%, respectively, of T cells expressing HLA-DP (Figures 1A and 1B). Given the heterogeneity of HLA-DP expression on $CD3^+CD8^+$ T cells, HLA-DP expression was investigated at different stages

of $CD8^+$ T cell differentiation.[36–38] Following the exclusion of naive ($CCR7^+CD45RA^+$) T cells, KLRG1 and CD127 were used to identify $CD127^+$ $KLRG1^-$ memory precursor cells (MPECs), $CD127^+$ $KLRG1^+$ double-positive effector cells (DPECs), and $CD127^-$ $KLRG1^{-/+}$ effector cells/early effector cells (ECs/EECs) (Figure 1C). Naive $CD8^+$ T cells contained the lowest frequencies of HLA-DP^+ T cells. HLA-DP^+ cells were increased within $CD127^+$ MPEC and DPEC $CD8^+$ T cell subsets, with medians of 17.4% and 25.7%, respectively, and the highest frequencies of HLA-DP^+ cells were observed within $CD127^-$ EC/EEC T cell subsets, with a median of 85.8% (Figure 1D). The percentages of HLA-DP^+ $CD4^+$ T cells closely followed the differentiation status observed for $CD8^+$ T cells, albeit at lower frequencies (Figure S1A). Taken together, these data demonstrate that HLA-DP, but not HLA-DQ or HLA-DR, can be significantly expressed on $CD8^+$ T cells, in particular on memory and differentiated EC/EEC T cell subsets.

HLA-DP is transcribed in $CD8^+$ T cells and co-localizes with markers of immune cell differentiation

To further characterize $CD8^+$ T cell subpopulations that expressed HLA-DP, single-cell RNA sequencing (scRNA-seq) was performed. Given the differences in HLA-DP expression between $CD127^+$ and $CD127^-$ T cells, $CD8^+$ $CD127^+$ HLA-DP^-, $CD8^+$ $CD127^+$ HLA-DP^+, and $CD8^+$ $CD127^-$ HLA-DP^+ cells were isolated from three healthy donors. In total, scRNA-seq data of 13,000 T cells from all three sorted $CD8^+$ T cell populations were included and projected in two dimensions using uniform manifold approximation and projection (Figure 2A). Within these cells, unsupervised clustering identified 14 different $CD8^+$ T cell clusters, numbered 0 to 13. Based on the most highly differentially expressed genes (DEGs) associated with T cell differentiation, clusters were manually annotated. Four clusters (2, 7, 9, and 11) were marked by the expression of *CCR7*, *SELL* (CD62L), *LEF1*, and *TCF7* and therefore noted as naive T cell clusters. Cluster 10 was characterized by upregulation of T cell memory genes (*KLF6*, *DUSP1*, *FOS*, *IL-7R*), but did not present *KLRG1* transcripts, and hence was noted as an MPEC T cell cluster. Two clusters (0 and 1) expressed memory genes and showed transcription of cytotoxic markers; given these characteristics and the expression of *IL-7R* and *KLRG1*, these clusters were assigned to DPEC T cells. Four clusters (3, 4, 6, and 8) highly expressed effectors/cytotoxic genes such as *PRF1*, *GNLY*, and *FGFBP2* and were annotated as EC/EEC T cells. One cluster (5) exhibited high expression of *KLRB1, NCR3, RORC*, and *ZBTB16*, which are characteristics of mucosal-associated invariant T cells (Figure 2B). Clusters 12 and 13 included less than 100 cells and were therefore excluded from further analyses. In sum, five $CD8^+$ T cell subpopulations were identified, four of which (naive, MPECs, DPECs, and ECs/EECs) were used for further analysis.

When assessing the expression of HLA-II genes, we observed only minor expression of *HLA-DQA1* and *HLA-DRA* transcripts in the individual T cell subpopulations, while *HLA-DPA1* was highly transcribed in $CD8^+$ T cells (Figures 2C, S2A, and S2B), consistent with the results from HLA-II protein expression analyses by flow cytometry. In line with this, *HLA-DPA1* and *HLA-DPB1* were furthermore significantly upregulated within the DPEC and EC/EEC clusters (Figure S2A). The scRNA-seq analyses also supported that *HLA-DP* was co-expressed with transcripts of markers observed upon repeated

immunological stimulation and immune cell differentiation, including CD57 (*B3GAT1*), CX3C-chemokine receptor 1 (*CX3CR1*), and the inhibitory receptor *TIGIT*. Furthermore, common transcriptional signatures found in *HLA-DP*$^+$ CD8$^+$ T cells were high levels of T-bet (*T-box transcription factor TBX21*) and Eomesodermin (*Eomes*) (Figure S2B). Consistent with the gene expression data, subsequent flow cytometry analyses showed that CD8$^+$ HLA-DP$^+$ T cells expressed significantly higher levels of CD57, CX3CR1, TIGIT, and the transcription factors T-bet and Eomes compared to HLA-DP$^-$ CD8$^+$ T cells (Figure 2D). A DEG analysis comparing the transcriptional profiles of HLA-DP$^-$ vs. HLA-DP$^+$ CD8$^+$ T cells within the EC/EEC clusters further showed that HLA-DP$^+$ CD8$^+$ T cells express markers of T cell exhaustion (*LAG3* and *TOX*) and T cell activation (*CD2* and *ITGAL*), as well as *SLAMF7* that encodes for the NK cell receptor ligand CRACC (Figure S2C). Taken together, these data show that *HLA-DPA1* and *HLA-DPB1* mRNA is transcribed by CD8$^+$ T cells of healthy individuals and that the expression of HLA-DP is correlated with markers linked to CD8$^+$ T cell maturation and differentiation.

HCMV infection is associated with significant upregulation of HLA-DP expression on CD8$^+$ T cells

The above data demonstrated preferential expression of HLA-DP on CD127$^-$ CD8$^+$ T cells with features associated with T cell maturation and differentiation. As previous studies have described the ability of HCMV infection to drive CD8$^+$ T cells toward a differentiated CD127$^-$ phenotype,[39,40] we investigated whether HLA-DP expression on CD8$^+$ T cells was associated with HCMV infection by stratifying results according to donors' HCMV serostatus. Total CD8$^+$ T cells from HCMV-seropositive donors exhibited high frequencies of HLA-DP$^+$ cells, with a median of 59.3%, whereas CD8$^+$ T cells from HCMV-seronegative donors had significantly lower values, with a median of 13% (Figure 3A). To determine temporal associations between HLA-DP expression and HCMV infection, we characterized longitudinally peripheral blood mononuclear cell samples acquired from renal transplant recipients experiencing primary HCMV infection.[37] CD8$^+$ T cells collected prior to transplantation (TX) from HCMV$^-$ individuals exhibited low levels of HLA-DP$^+$ CD8$^+$ T cells, but HLA-DP frequencies significantly increased on CD8$^+$ T cells from samples collected ~1 month after HCMV seroconversion and ~18 months after TX (Figure 3B). Frequencies of HLA-DP$^+$ CD8$^+$ T cells were highest in EC/EEC T cell populations from HCMV$^+$ as well as HCMV$^-$ individuals. However, HLA-DP$^+$ CD8$^+$ T cells were more frequent within all CD8$^+$ effector T cell subpopulations in HCMV$^+$ individuals, and significantly higher frequencies of HLA-DP$^+$ CD8$^+$ T cells were observed within MPEC and DPEC CD8$^+$ T cell subsets in HCMV-seropositive compared to -seronegative individuals (Figures 3C and S3A). To further investigate associations between HCMV infection and HLA-DP expression, we assessed HLA-DP expression on HCMV-specific CD8$^+$ T cells using an HLA-A*02:01-NLVPMVATV tetramer. In line with the increased HLA-DP expression upon primary HCMV infection, the majority of HCMV-specific CD8$^+$ T cells showed high HLA-DP frequencies (Figure 3D). Taken together, these data demonstrate that upon HCMV infection, HLA-DP expression on CD8$^+$ T cells further increased, in particular on those CD8$^+$ T cells transitioning from naive to fully differentiated effector populations.

The activating NK cell receptor NKp44 binds to some, but not all, HLA-DP molecules expressed on CD8+ T cells

Some HLA-DP molecules can serve as ligands for the activating NK cell receptor NKp44, while others do not bind NKp44,[34] providing a model to investigate the impact of NKp44/HLA-DP interactions on the regulation of $CD8^+$ T cells. "HLA-DP201" (encoded by *HLA-DPA1*01:03* and *HLA-DPB1*02:01*) and "HLA-DP401" (encoded by *HLA-DPA1*01:03* and *HLA-DPB1*04:01*), which is the most frequent HLA-DP haplotype in White populations,[41] serve as functional ligands for NKp44, while "HLA-DP301" (encoded by *HLA-DPA1*01:03* and *HLA-DPB1*03:01*) and "HLA-DP501" (encoded by *HLA-DPA1*02:02* and *HLA-DPB1*05:01*), two less frequent haplotypes, do not bind NKp44.[34] We initially investigated whether NKp44 can bind to HLA-DP molecules expressed on $CD8^+$ T cells from $HCMV^+$ individuals. Using a recombinant human NKp44-Fc construct, we observed that HLA-DP^+ $CD8^+$ T cells showed significant NKp44-Fc binding, whereas HLA-DP $CD8^+$ T cells did not (Figure 4A). Next, we investigated functional consequences by co-incubating $NKp44^+$ NK cells with HLA-DP^+ $CD8^+$ T cells. NKp44 expression on peripheral-blood-derived NK cells was induced upon culture with interleukin (IL)-2 and IL-15 (Figures S4A and S4C). Co-culture of $NKp44^+$ NK cells with $CD8^+$ T cells expressing NKp44-binding HLA-DP molecules (i.e., HLA-DP401) resulted in NK cell activation, quantified by CD107a[42] expression and TNF production, whereas co-culture with $CD8^+$ T cells derived from individuals carrying exclusively NKp44 non-binding HLA-DP haplotypes, such as HLA-DP301, resulted in significantly lower NK cell activation (Figures 4B, 4C, and S4B). Furthermore, blocking of the interaction between $NKp44^+$ NK cells and $CD8^+$ T cells expressing NKp44-binding HLA-DP heterodimers using an NKp44 blocking antibody resulted in significantly decreased CD107a expression by $NKp44^+$ NK cells (Figure 4D). Given the observed degranulation of NK cells upon interaction between NKp44 and NKp44-binding HLA-DP molecules, we investigated the consequences for $CD8^+$ T cells using lactate dehydrogenase release as a measure of NK cell-mediated cytotoxicity. Co-incubation of NK cells and $CD8^+$ T cells resulted in significantly higher $CD8^+$ T cell lysis when $CD8^+$ T cells were enriched for HLA-DP (Figure 4E). Taken together, these *in vitro* data show that $NKp44^+$ NK cells can functionally respond to HLA-DP^+ $CD8^+$ T cells from donors encoding NKp44-binding HLA-DP haplotypes.

Hyper-expansion of CD8+ T cell clones in individuals encoding NKp44 non-binding HLA-DP antigens

To investigate *in vivo* consequences of interactions between $NKp44^+$ NK cells and HLA-DP-expressing $CD8^+$ T cells, we compared HLA-DP expression on $CD8^+$ T cells in HCMV-seropositive individuals encoding either only NKp44-binding HLA-DP haplotypes (e.g., HLA-DP201 and HLA-DP401) or exclusively NKp44 non-binding HLA-DP haplotypes (e.g., HLA-DP301 and HLA-DP501). Frequencies of HLA-DP^+ cells within the total $CD8^+$ T cell population were significantly lower in individuals carrying two NKp44-binding HLA-DP haplotypes (median: 52.1%, range: 26.5%–67.2%) compared to individuals carrying two NKp44 non-binding HLA-DP haplotypes (median: 81.7%, range: 70.9%–93.6%, $p = 0.0095$) (Figure 5A). To further investigate potential differences in the T cell receptor (TCR) Vβ usage and expansion of $CD8^+$ HLA-DP^+ T cells between individuals encoding NKp44-binding and NKp44 non-binding HLA-DP antigens, we employed a panel of 24 TCR

Vβ antibodies. Notably, individuals exclusively encoding NKp44 non-binding HLA-DP heterodimers exhibited significantly more hyper-expanded (relative TCR Vβ contribution >10%) chains ranging from 11% to 43.6% of all $CD8^+$ $HLA\text{-}DP^+$ T cells than individuals encoding for NKp44-binding HLA-DP antigens ($p = 0.0476$) (Figures 5B; Table 1; Table S1). Furthermore, within individuals expressing only NKp44-binding HLA-DP haplotypes, more frequent TCR Vβ hyper-expansion in $HLA\text{-}DP^-$ compared to $HLA\text{-}DP^+$ EC/EEC $CD8^+$ T cells was observed (Figure S5A), indicating that TCR Vβ chain expansion of $CD8^+$ T cells was more restricted in individuals encoding HLA-DP molecules that enabled binding of NKp44.

To confirm the observed differences in TCR Vβ chain expansion on the level of $CD8^+$ T cell clones, TCR sequencing from sorted $HLA\text{-}DP^+$ $CD8^+$ T cells of individuals carrying two HLA-DP-NKp44 binder vs. two HLA-DP-NKp44 non-binder haplotypes was performed. TCR sequencing analyses revealed highly clonal T cell repertoires and lower Shannon indexes (Figure S5B) in individuals exclusively carrying NKp44 non-binding HLA-DP haplotypes compared to individuals carrying NKp44-binding HLA-DP haplotypes. In line with the lower HLA-DP expression by naive cells, no significant differences in T cell clonality (size of 10 most frequent T cell clones) were observed in naive $CD8^+$ T cells between individuals encoding two NKp44-binding vs. two NKp44 non-binding HLA-DP antigens (Figure 5C). In contrast, both $CD127^+$ (MPEC/DPEC) and $CD127^-$ (EC/EEC) $CD8^+$ T cells from individuals with two NKp44 non-binding HLA-DP antigens showed significantly larger expansion of $CD8^+$ T clones (size of the top 10 clones) compared to individuals carrying two NKp44-binding HLA-DP haplotypes (Figure 5C). Taken together, these data demonstrate that effector $CD8^+$ T cells in $HCMV^+$ individuals exclusively carrying NKp44 non-binding HLA-DP haplotypes exhibit more frequent clonal hyper-expansion of $CD8^+$ T cells than do $CD8^+$ T cells in individuals carrying NKp44-binding HLA-DP haplotypes, consistent with $NKp44^+$ NK cell-mediated regulation of $CD8^+$ T cell expansion and clonality.

DISCUSSION

Regulation of T cell responses is critical to secure protection from viral infections while preventing excessive T cell expansion that can cause immunopathology, including autoimmune diseases.[43] The precise mechanisms involved in regulation of $CD8^+$ T cell expansion and in limiting hyper-expansion of clonal $CD8^+$ effector T cells are insufficiently understood, but recent studies, predominantly using mouse models, have revealed a role for NK cells in limiting T cell expansion and preventing T cell-mediated autoimmunity.[11,13] In this study, we show that human $CD8^+$ T ECs express HLA-DP molecules and report a functional HLA-DP-dependent interaction between $NKp44^+$ NK cells and $HLA\text{-}DP^+$ $CD8^+$ T cells that was associated with clonal expansion of $CD8^+$ T cells *in vivo* in $HCMV^+$ individuals exclusively carrying NKp44 non-binding HLA-DP haplotypes. These studies provide a molecular mechanism for NK cell-mediated regulation of $HLA\text{-}DP^+$ $CD8^+$ T cells in humans with implications for T cell-mediated autoimmune diseases that are associated with HLA-DP haplotypes encoding antigens that are unable to bind NKp44.

Under physiological conditions, constitutive expression of HLA-II molecules is observed on B cells and APCs; however, HLA-II molecules can be upregulated on other immune cells upon cytokine exposure and activation.[35] While HLA-DR serves as a well-characterized T cell activation marker,[44] our data show that HLA-DP is expressed on the surface of resting T cells, particularly on differentiated $CD8^+$ T cells, and to a lesser extent on $CD4^+$ T cells. HLA-DP expression on T cells was transcriptionally regulated and not a consequence of cell-to-cell transfer during trogocytosis,[45] as scRNA-seq data analysis revealed that *HLA-DP* was highly transcribed in $CD8^+$ T ECs, while *HLA-DR* and *HLA-DQ* mRNA transcription was low. In line with the expression of HLA-DP on differentiated $CD8^+$ T cells, HLA-DP expression on $CD8^+$ T cells was significantly higher in $HCMV^+$ individuals and induced after HCMV infection, as higher frequencies of $HLA\text{-}DP^+$ $CD8^+$ T cells were observed in individuals early following HCMV seroconversion. Currently it remains unknown whether other viral infections might also lead to HLA-DP upregulation on $CD8^+$ T cells. However, previous studies have shown that viral infections can induce phenotypical and epigenetic modification to immune cells[46–49] and, in particular, that HCMV infection confers a characteristic transcriptional and protein expression phenotype to $CD8^+$ T cells,[39,40] as well as NK cells.[49,50] Hallmarks of terminally differentiated effector memory T cells induced by HCMV are high expression of CD57, KLRG1, and CX3CR1 and transcription of T-bet and Eomes, as well as downregulation of CD127,[51] and the expansion of these terminally differentiated T cells has been associated with immunosenescence in older age.[40] Using scRNA-seq and phenotypic characterization of $CD8^+$ T cell populations, we observed that HLA-DP was co-expressed with other markers of T cell differentiation, including T-bet, Eomes, CD57, and CX3CR1, identifying HLA-DP as a marker of highly differentiated $CD8^+$ T cells that is induced by HCMV infection.

Studies in mice have shown that NK cells can control the expansion of T cells in a contact-dependent, receptor/ligand-mediated process, with important consequences for the outcome of T cell-mediated diseases, including autoimmune diseases.[11,13,52] For example, enhanced NK cell-mediated elimination of T cells was beneficial in a model of experimental autoimmune encephalomyelitis[11] and reduced virus-induced autoimmunity.[13] Furthermore, NK cells expressing the activating NCR NCR1 have been shown to suppress $CD8^+$ T cell expansion upon lymphocytic choriomeningitis virus infection,[53] preventing the induction of diabetes in mice.[52] Here, we show that human NK cells, through the activating NCR NKp44 (NCR2, which is not expressed in mice), can regulate the expansion of $HLA\text{-}DP^+$ $CD8^+$ T cells in an HLA-DP antigen-dependent process. Previous studies have demonstrated that NKp44 can bind to a subset of HLA-DP molecules,[34] including molecules encoded by the common HLA-DP haplotypes *HLA-DPA1*01:03~DPB1*04:01* (HLA-DP401) and *HLA-DPA1*01:03~DPB1*02:01* (HLA-DP201) (with allele frequencies in White people of 40% and 10%, respectively),[41] while no binding of NKp44 was observed to *HLA-DPA1*01:03~DPB1*03*:01 (HLA-DP301) and *HLA-DPA1*02:02~DPB1*05*:01 (HLA-DP501), which are much less frequent in White populations with allele frequencies of 4.2% and 0.8%, respectively.[41] Here, we show that $NKp44^+$ NK cells are more strongly activated when co-incubated with $CD8^+$ T cells from donors that carry NKp44-binding HLA-DP haplotypes than with donors that carry NKp44 non-binding HLA-DP haplotypes. This interaction was dependent on NKp44, as NKp44 blocking decreases NK

cell degranulation. Interestingly, $CD8^+$ T cells from those rare individuals that encode exclusively NKp44 non-binding HLA-DP antigens included significantly more $HLA\text{-}DP^+$ cells and exhibited significantly stronger clonal $CD8^+$ T cell expansion than $CD8^+$ T cells from individuals encoding NKp44-binding HLA-DP antigens, suggesting a regulation of $NKp44^+$ NK cells on $CD8^+$ T cells. Future studies on larger populations of individuals encoding NKp44-binding and NKp44 non-binding HLA-DP antigens will be required to investigate the impact of additional variables affecting $CD8^+$ T cell expansion, including HLA-I genotypes, expression of ligands for other NK cell receptors, such as PD-1/PD-L1,[22] age, and other viral co-infections.

HLA-DP haplotype diversity is linked to the genetic predisposition for several autoimmune diseases,[54,55] including autoimmune hepatitis (AIH)[56] and type 1 diabetes (T1D),[31,32] two autoimmune diseases with a well-established role of T cells in their pathogenesis.[57,58] HCMV infection represents an important risk factor for the development of T1D.[59] Importantly, *HLA-DPB1*03:01*, which encodes the β-chain of the NKp44 non-binding HLA-DP molecule, represents a risk allele for T1D,[32] while *HLA-DPB1*04:01*, which encodes the β-chain of the NKp44-binding HLA-DP molecule HLA-DP401, has been reported to be protective.[31] Similarly, the rs9277534G SNP in the 3′ untranslated region of the HLA-DP β-chain, which is associated with the expression of *HLA-DPB1*03:01* and *HLA-DPB1*05:01*,[58] represents a significant risk SNP for AIH, while the rs9277534A SNP, associated with the expression of *HLA-DPB1*04:01* and *HLA-DPB1*02:01*, is protective in AIH.[56] Failure to restrict clonal $CD8^+$ T cell expansion by NKp44/HLA-DP interactions in individuals who have only NKp44 non-binding HLA-DP risk haplotypes might therefore contribute to T cell-mediated autoimmune responses, providing a potential molecular mechanism for the described HLA-DP allele disease associations. While circulating peripheral blood NK cells do not express NKp44 *ex vivo*, it was reported that hepatic NK cells exhibit high frequencies of $NKp44^+$ NK cells,[54] and liver tissues have been proposed as a site for the removal of apoptotic T cells.[60] In conclusion, we identified a functional interaction between human $NKp44^+$ NK cells and $HLA\text{-}DP^+$ $CD8^+$ T cells that depended on the haplotype-encoding HLA-DP, associated with an HLA-DP-dependent restriction of clonal $CD8^+$ T cell expansion. The NKp44/HLA-DP pathway might therefore represent a target to modulate the expansion of $CD8^+$ T ECs by immune-therapeutic interventions.

Limitation of the study

A limitation of this study is related to the sample size, as individuals carrying exclusively NKp44 non-binding HLA-DP haplotypes are rare in White populations. Future studies on larger populations of individuals encoding NKp44-binding and NKp44 non-binding HLA-DP antigens will be required to investigate the impact of additional variables impacting $CD8^+$ T cell expansion.

STAR★METHODS

RESOURCE AVAILABILITY

Lead contact—Further information and request for resources and reagents should be directed to and will be fulfilled by the lead contact, Marcus Altfeld (marcus.altfeld@leibniz-liv.de).

Materials availability—This study did not generate new unique reagents.

Data and code availability—All data are available in the main text, supplemental figures/tables, or data repositories, as of the date of publication. The RNA-seq data used in Figure 2 are available at ArrayExpress: accession number is available in the key resources table. The $CD8^+$ T cells TCR sequencing data used in Figure 5 are available at ENA: accession number is available in the key resources table. This paper does not report original code. Any additional information required to reanalyze the data reported in this paper is available from the lead contact upon request.

EXPERIMENTAL MODEL AND STUDY PARTICIPANT DETAILS

Peripheral blood samples were obtained from healthy human donors (healthy Hamburg cohort). All donors gave written informed consent. The study (PV4780) was approved by the ethical commission “Ärztekammer” Hamburg. In addition, peripheral blood from renal transplant recipients ($n = 6$) were obtained from the Academic Medical Center, Amsterdam. The donors provided written informed consent and the medical ethics committee of the Academic Medical Center, Amsterdam, The Netherlands approved the study. Sample sizes are reported in the respective figure legends. Information regarding age, sex and gender of the study participants were not fully available.

METHOD DETAILS

Isolation and freezing of PBMCs—Peripheral blood mononuclear cells (PBMCs) were isolated from healthy individuals′ blood using density gradient centrifugation (Capricorn Scientific). Freshly isolated PBMCs were immediately used for experiments or cryopreserved for subsequent analysis in heat inactivated fetal bovine serum (FBS) (Capricorn Scientific) supplemented with 10% (v/v) dimethyl sulfoxide (DMSO) (Sigma-Aldrich) and stored in liquid nitrogen.

HCMV serostatus determination—Plasma levels of anti-cytomegalovirus IgG were determined using a commercially available enzyme-linked immunosorbent assay (human anti-cytomegalovirus IgG ELISA kit, Abcam) following manufacturer′s instruction. Absorbance was measured at 450 nm at a Safire2 microplate reader (Tecan, Männedorf, Switzerland) using the Magellan software version 6.1.

Cell staining, flow cytometry, cell sorting—Prior to staining PBMCs were washed in PBS (Sigma-Aldrich). Where reported, cells were stained with a major histocompatibility complex (MHC) class I labeled tetramer for 15 min at 37°C/Dark or with Beta Mark TCR Vbeta Repertoire Kit (Beckman Coulter). LIVE/DEAD fixable Near-IR Dead cells staining

kit (Invitrogen) and an optimized panel of directly conjugated antibodies were used to identify surface markers and to exclude dead cells. Staining was performed for 20 min at RT/Dark. Cells were then fixed with 4% paraformaldehyde (PFA) for 30 min at 4°C or fixed/permeabilized using BD Cytofix/Cytoperm Fixation and Permeabilization Solution (BD Biosciences) or FoxP3/Transcription Factor Staining Buffer Set (eBioscience). Transcription factors antibodies were incubated for 1h at RT/Dark. Cells were then washed and measured with a Cytex Aurora 5 Laser and analyzed using FlowJo 10.8 software (BD Biosciences). For cell sorting, PBMCs were stained with the indicated antibodies, left unfixed, stored on ice and sorted using a FACSAria Fusion (BD Biosciences) device in the core facility Fluorescence Cytometry at the Leibniz Institute of Virology, Hamburg. The antibodies used for staining are shown in key resources table.

Single-cell RNA sequencing

Preparation of scRNA-Seq, CITE-Seq libraries: Freshly isolated PBMCs from three healthy individuals were stained using surface markers antibodies and CITE-Seq antibodies either barcoded using in-house (CD45 (BioLegend, USA) conjugated with the barcoding oligonucleotides CAGGCG – CACTCA) as previously described[61] or using TotalSeq A antibodies. (BioLegend, USA). (key resources table). $CD8^+$ IL-7R+ HLA-DP−, IL-7R+ HLA-DP+, IL-7R− HLA-DP+ cells were FACS-sorted, using a FACSAria fusion (BD Biosciences). FACS-sorted cells were washed once with autoMACS Running Buffer (Miltenyi Biotec) and resuspended in PBS. 25.000 cells were used for GEM generation through the 10X Chromium Controller using the 10x V3 B Chip GEM generation kit (10x Genomics, USA).

Sequencing: The scRNA libraries were sequenced on an Illumina NextSeq or HiSeq 4000 to a minimum sequencing depth of 25,000 reads per cell using read lengths of 26 bp read 1, 8 bp i7 index, 98 bp read 2.

Single-cell raw data processing: The sequencing reads were process by cellranger (version 4.0.0, 10x Genomics, USA) and aligned against the reference genome provided by 10X (refdata-gex-GRCh38–2020-A). Further analysis steps were performed in R (version 4.2.0; The R Foundation for Statistical Computing, Vienna, Austria).

First, the cells from the 3 donors were demultiplexed into the $CD8^+$ CD127+ HLA-DP−, $CD8^+$ CD127+ HLA-DP+, and $CD8^+$ CD127-HLA-DP + populations based on their cell hashing hash tag oligo (HTO) data with HTODemux implemented in the Seurat[62] package (version 4.2.0). The HTODemux function first performs K-medoid clustering (K = #samples +1) on the normalized HTO expression data. Then for each CD45-tag the cluster with the lowest average expression was determined and a negative binomial distribution was fit to this cluster. Based on these distributions and a quantile of 0.99 each cell was classified into being positive or negative for each CD45-tag. Cells positive for more than one tag were classified as doublets and discarded.

The following filters were then applied to the cells of each demultiplexed sample individually Genes not observed in at least 1% of all cells were dropped. Low quality or damaged cells were excluded using a combination of multiple sample dependent

quality measures: minimum UMI count, minimum and maximum number of expressed genes and mitochondrial transcript percentage. Additionally, we filtered out doublet cell candidates using Scrublet[63] (version 0.2.3). To normalize the UMI counts we used Seurat's logNormalize method and identified the 2000 most highly variable genes (HVG) based on variance stabilizing transformation.

To perform joint analysis on all samples we applied Seurat's canonical correlation analysis data integration approach using 2,000 genes that appear in the HVG set of the maximum number of samples as anchors.

The batched corrected counts for all integration anchors were used as input for PCA. For UMAP embedding and graph-based shared nearest neighbor clustering we used the first 20 principal components. For the Louvain clustering algorithm we used a resolution of 0.4. Cluster marker detection was performed by differential gene expression analysis for each cluster against all remaining cells using logistic regression on the sample-wise normalized RNA matrices. We included the donor variable as covariate in the regression model and tested for significant differential expression against a null model with likelihood ratio test.

For differential expression analysis within clusters between groups we used Libra[64] in pseudobulk mode. Genes were deemed differentially expressed, if an adjusted *p* value below 0.05 and an average absolute log2 fold change above 0.25 was observed.

Isolation of human CD8 T and NK cells—Primary human CD8 T cells and NK cells were enriched from PBMCs using magnetic labeling and negative selection using the EasySep Human $CD8^+$ T cell enrichment kit (StemCell Technologies) and EasySep Human NK cell entichment kit (StemCell Technologies), respectively. Isolated CD8 T cells were directly used for experimental procedures. NK cells were cultured for 4–5 d at 37°C/5% CO_2 in RPMI-1640 supplemented with 10% FBS 10 ng mL^{-1} IL-15 and 250 U ml^{-1} IL-2 (PeproTech) at a concentration of 1×10^6 cells ml^{-1} to induce NKp44 expression.

NKp44-Fc construct staining of $CD8^+$ T cells—$CD8^+$ T cells were loaded with 100μM B2M peptide (sequence: FYLLYYTEFTPT[65]) for 2h at 37°C/5% CO. Cells were washed and stained with NKp44/Fc chimera (R&D) at a final concentration of 25 μg/ml for 30 min at 37°C/DARK. Cells were then washed with PBS and incubated F(ab)2-goat-*anti*-human-Fc R-PE (Life Technologies) antibody for 20 min at RT. Cells were washed twice with PBS and stained with surface antibodies for 20 min at RT and subsequently fixed with PBS/4% PFA for 30 min at 4°C.

NK cell degranulation assay and NKp44 blocking—On the day of the degranulation CD8 T cells were enriched from PBMCs (as described above), washed twice with RPMI-1640 supplemented with 10% FBS. Isolated NK cells (5×10^4 cells per well) were co-incubated at an effector/target ratio of 1:5 with CD8 T cells O.N at 37°C in RPMI 1640 supplemented with 10% FBS 10 ng mL^{-1} IL-15 and 250 U ml^{-1} IL-2 (PeproTech) in presence of anti-CD107a BV421 (BioLegend) and 2.5 μg/ml of Brefeldin A (BFA). For blocking experiments, isolated NK cells were pre-incubated with 25 μg/ml of Ultra-LEAF Purified anti-human CD336 (NKp44) Antibody (BioLegend) or 25 μg/ml of Ultra-LEAF

Purified Mouse IgG1, κ Isotype Ctrl Antibody (BioLegend) for 15 min at RT in RPMI 1640 supplemented with 10% FBS 10 ng mL^{-1} IL-15 and 250 U ml^{-1} IL-2 (PeproTech). After pre-incubation, NK cells were incubated with $CD8^+$ T at an effector/target ratio of 1:5 for 5h at 37°C in complete medium and in presence of blocking antibodies, anti-CD107a BV421 (BioLegend) and 2.5 μg/ml of Brefeldin A (BFA).

HLA-DP$^+$ CD8$^+$ T cell enrichment and NK cell killing—On the day of the experiment, $CD8^+$ T cells were enriched from PBMCs (as described above). Subsequently, $CD8^+$ T cells were stained with HLA-DP-PE conjugated antibody (BD Biosciences) and incubated for 15 min, in the dark at RT. Cells were then washed and resuspended with Anti-PE MicroBeads (Miltenyi Biotec) following the manufacturer's recommendations. Cells were subsequently washed and HLA-DP depleted/enriched with two rounds of magnetic separation using MS Columns and a OctoMACS Separator (Miltenyi Biotec) following the manufacturer's recommendations. $CD8^+$ depleted/enriched for HLA-DP were successively washed, counted and resuspended at ratio of 1:1 with NK cells for 1 day at 37°C in RPMI 1640 supplemented with 10% FBS 10 ng mL^{-1} IL-15 and 250 U ml^{-1} IL-2 (PeproTech). At the end of the co-incubation, NK cell mediated-cytotoxicity was measured directly analyzing the supernatants using CyQUANT LDH Cytotoxicity Assay Kit (Invitrogen).

TCR sequencing of CD8$^+$ T cells

Cell sorting: Freshly isolated PBMCs from three healthy individuals were stained with surface markers antibodies. $CD8^+$ T cells were sorted as Naive, IL-7R+ and IL-7R− $CD8^+$ T cells using a FACSAria fusion (BD Biosciences).

gDNA isolation: Genomic DNA from sorted $CD8^+$ T cells was isolated using the QIAmp DNA Micro Kit (Qiagen, Hilden, Germany) according to the manufacturer´s instructions.

TCR immunosequencing and data analysis: We identified $CD8^+$ T cell clonotypes using next-generation immunosequencing.[66,67] In brief, we amplified the V(D)J rearranged TRB loci from 250 to 500 ng gDNA of sorted $CD8^+$ T cells in a two-step multiplex PCR using the BIOMED2-TRB primer pool.[68,69] Illumina-tagged and barcoded amplicons were purified using the NucleoSpinGel and PCR Clean-up kit (Macherey-Nagel, Düren, Germany), quantified on the Qubit platform (QIAGEN, Hilden, Germany), pooled to a final library concentration of 4 nM and quality controlled on an Agilent 2100 Bioanalyzer (Agilent Technologies, Böblingen, Germany). Sequencing was performed on an Illumina MiSeq (paired-end, 2 9301-cycles) at an average sequencing depth of 56,000 reads. Rearranged TRB loci were annotated from raw reads using the MiXCR frame-work 3.0.13[70] and the default MiXCR library as reference for sequence alignment. Non-productive reads and sequences with less than 2 read counts were not considered for further analysis. Each unique complementarity-determining region 3 (CDR3) nucleotide sequence was defined as one clone. All Samples were normalized to a read depth of 30,000. Broad repertoire metrics (clonality, diversity, richness) were analyzed as previously described.[71,72] All analyses and data plotting of TCR sequencing data were performed using R version 4.1.12.

HLA genotyping—HLA typing was performed using a targeted next generation sequencing (NGS) method. Briefly, locus-specific primers were used to amplify a total of 26 polymorphic exons of HLA-A & B (exons 1 to 4), C (exons 1 to 5), E (exon 3), DPA1 (exon 2), DPB1 (exons 2 to 4), DQA1 (exon 1 to 3), DQB1 (exons 2 & 3), DRB1 (exons 2 & 3), and DRB3/4/5 (exon 2) genes with Fluidigm Access Array (Fluidigm Corporation, South San Francisco, CA 94080 USA). The 26 Fluidigm PCR amplicons were pooled and subjected to sequencing on an Illumina MiSeq sequencer (Illumina, San Diego, CA 92122 USA). HLA alleles and genotypes were called using the Omixon HLA Explore (version 2.0.0) software (Omixon Biocomputing Ltd., Budapest, Hungary).

QUANTIFICATION AND STATISTICAL ANALYSIS

Statistical analysis were performed using GraphPad Prism 9 (GraphPad Software). The non-parametric two-tailed Wilcoxon matched pairs signed rank test and two-tailed Friedman test with post-hoc Dunn′s multiple comparison were used to compare differences between paired conditions. The non-parametric Mann-Whitney test was applied to compare differences between unpaired conditions. A two-tailed Fisher′s Exact Test was used to calculate the statistical significance for the TCRvβ expansion, while Ordinary 1-way ANOVA was used to compare differences between TCR clones. Values of $p < 0.5$ were considered significant. The statistical details and exact p values can be found in the figure legends.

Supplementary Material

Refer to Web version on PubMed Central for supplementary material.

ACKNOWLEDGMENTS

We would like to thank the donors and coordinators of the Hamburg Healthy Cohort and the Core Facility for Fluorescence Cytometry at the Leibniz Institute of Virology (LIV). This work was funded by the European Research Council (ERC) under the European Union's Horizon 2020 research and innovation programme (grant agreement no. 884830) and by the DFG (SFB1192 and BU3630-3-1). This project has been funded in whole or in part with federal funds from the Frederick National Laboratory for Cancer Research under contract no. 75N91019D00024. The content of this publication does not necessarily reflect the views or policies of the Department of Health and Human Services, nor does mention of trade names, commercial products, or organizations imply endorsement by the US government. This research was supported in part by the Intramural Research Program of the NIH, Frederick National Lab, and Center for Cancer Research. The graphical abstract was created using BioRender.com.

REFERENCES

1. Moretta A, Bottino C, Mingari MC, Biassoni R, and Moretta L (2002). What is a natural killer cell? Nat. Immunol. 3, 6–8. 10.1038/ni0102-6. [PubMed: 11753399]
2. Vivier E, Tomasello E, Baratin M, Walzer T, and Ugolini S (2008). Functions of natural killer cells. Nat. Immunol. 9, 503–510. 10.1038/ni1582. [PubMed: 18425107]
3. Jost S, and Altfeld M (2013). Control of Human Viral Infections by Natural Killer Cells. Annu. Rev. Immunol. 31, 163–194. 10.1146/annurev-immunol-032712-100001. [PubMed: 23298212]
4. Waggoner SN, Cornberg M, Selin LK, and Welsh RM (2011). Natural killer cells act as rheostats modulating antiviral T cells. Nature 481, 394–398. 10.1038/nature10624. [PubMed: 22101430]
5. Waggoner SN, Daniels KA, and Welsh RM (2014). Therapeutic Depletion of Natural Killer Cells Controls Persistent Infection. J. Virol. 88, 1953–1960. 10.1128/JVI.03002-13. [PubMed: 24284324]

6. Lang PA, Lang KS, Xu HC, Grusdat M, Parish IA, Recher M, Elford AR, Dhanji S, Shaabani N, Tran CW, et al. (2012). Natural killer cell activation enhances immune pathology and promotes chronic infection by limiting CD8 + T-cell immunity. Proc. Natl. Acad. Sci. USA 109, 1210–1215. 10.1073/pnas.1118834109. [PubMed: 22167808]
7. Cook KD, and Whitmire JK (2013). The Depletion of NK Cells Prevents T Cell Exhaustion to Efficiently Control Disseminating Virus Infection. J. Immunol. 190, 641–649. 10.4049/JIMMUNOL.1202448. [PubMed: 23241878]
8. Rydyznski C, Daniels KA, Karmele EP, Brooks TR, Mahl SE, Moran MT, Li C, Sutiwisesak R, Welsh RM, and Waggoner SN (2015). Generation of cellular immune memory and B-cell immunity is impaired by natural killer cells. Nat. Commun. 6, 6375–6414. 10.1038/ncomms7375. [PubMed: 25721802]
9. Rydyznski CE, Cranert SA, Zhou JQ, Xu H, Kleinstein SH, Singh H, and Waggoner SN (2018). Affinity Maturation Is Impaired by Natural Killer Cell Suppression of Germinal Centers. Cell Rep. 24, 3367–3373.e4. 10.1016/j.celrep.2018.08.075. [PubMed: 30257198]
10. Takeda K, and Dennert G (1993). The development of autoimmunity in C57BL/6 lpr mice correlates with the disappearance of natural killer type 1-positive cells: evidence for their suppressive action on bone marrow stem cell proliferation, B cell immunoglobulin secretion, and autoimmune sy. J. Exp. Med. 177, 155–164. 10.1084/jem.177.1.155. [PubMed: 8418197]
11. Lu L, Ikizawa K, Hu D, Werneck MBF, Wucherpfennig KW, and Cantor H (2007). Regulation of Activated CD4+ T Cells by NK Cells via the Qa-1–NKG2A Inhibitory Pathway. Immunity 26, 593–604. 10.1016/j.immuni.2007.03.017. [PubMed: 17509909]
12. Schuster IS, Sng XYX, Lau CM, Powell DR, Weizman OE, Fleming P, Neate GEG, Voigt V, Sheppard S, Maraskovsky AI, et al. (2023). Infection induces tissue-resident memory NK cells that safeguard tissue health. Immunity 56, 531–546.e6. 10.1016/J.IMMUNI.2023.01.016. [PubMed: 36773607]
13. Schuster IS, Wikstrom ME, Brizard G, Coudert JD, Estcourt MJ, Manzur M, O'Reilly LA, Smyth MJ, Trapani JA, Hill GR, et al. (2014). TRAIL+ NK Cells Control CD4+ T Cell Responses during Chronic Viral Infection to Limit Autoimmunity. Immunity 41, 646–656. 10.1016/j.immuni.2014.09.013. [PubMed: 25367576]
14. Crome SQ, Lang PA, Lang KS, and Ohashi PS (2013). Natural killer cells regulate diverse T cell responses. Trends Immunol. 34, 342–349. 10.1016/J.IT.2013.03.002. [PubMed: 23601842]
15. Schuster IS, Coudert JD, Andoniou CE, and Degli-Esposti MA (2016). "Natural Regulators": NK Cells as Modulators of T Cell Immunity. Front. Immunol. 7, 235. 10.3389/fimmu.2016.00235. [PubMed: 27379097]
16. Pallmer K, and Oxenius A (2016). Recognition and Regulation of T Cells by NK Cells. Front. Immunol. 7, 251. 10.3389/fimmu.2016.00251. [PubMed: 27446081]
17. Waggoner SN, Taniguchi RT, Mathew PA, Kumar V, and Welsh RM (2010). Absence of mouse 2B4 promotes NK cell–mediated killing of activated CD8+ T cells, leading to prolonged viral persistence and altered pathogenesis. J. Clin. Invest. 120, 1925–1938. 10.1172/JCI41264. [PubMed: 20440077]
18. Soderquest K, Walzer T, Zafirova B, Klavinskis LS, Polić B, Vivier E, Lord GM, and Martín-Fontecha A (2011). Cutting Edge: CD8+ T Cell Priming in the Absence of NK Cells Leads to Enhanced Memory Responses. J. Immunol. 186, 3304–3308. 10.4049/jimmunol.1004122. [PubMed: 21307295]
19. Xu HC, Grusdat M, Pandyra AA, Polz R, Huang J, Sharma P, Deenen R, Köhrer K, Rahbar R, Diefenbach A, et al. (2014). Type I Interferon Protects Antiviral CD8+ T Cells from NK Cell Cytotoxicity. Immunity 40, 949–960. 10.1016/j.immuni.2014.05.004. [PubMed: 24909887]
20. Crouse J, Bedenikovic G, Wiesel M, Ibberson M, Xenarios I, Von Laer D, Kalinke U, Vivier E, Jonjic S, and Oxenius A (2014). Type I Interferons Protect T Cells against NK Cell Attack Mediated by the Activating Receptor NCR1. Immunity 40, 961–973. 10.1016/j.immuni.2014.05.003. [PubMed: 24909889]
21. Peppa D, Gill US, Reynolds G, Easom NJW, Pallett LJ, Schurich A, Micco L, Nebbia G, Singh HD, Adams DH, et al. (2013). Up-regulation of a death receptor renders antiviral T cells susceptible to NK cell–mediated deletion. J. Exp. Med. 210, 99–114. 10.1084/jem.20121172. [PubMed: 23254287]

22. Diniz MO, Schurich A, Chinnakannan SK, Duriez M, Stegmann KA, Davies J, Kucykowicz S, Suveizdyte K, Amin OE, Alcock F, et al. (2022). NK cells limit therapeutic vaccine–induced CD8 + T cell immunity in a PD-L1–dependent manner. Sci. Transl. Med. 14, 4670. 10.1126/scitranslmed.abi4670.

23. Zhang Y, Yan AW, Boelen L, Hadcocks L, Salam A, Gispert DP, Spanos L, Bitria LM, Nemat-Gorgani N, Traherne JA, et al. (2023). KIR-HLA interactions extend human CD8+ T cell lifespan in vivo. J. Clin. Invest. 133, e169496. 10.1172/JCI169496. [PubMed: 37071474]

24. Boelen L, Debebe B, Silveira M, Salam A, Makinde J, Roberts CH, Wang ECY, Frater J, Gilmour J, Twigger K, et al. (2018). Inhibitory killer cell immunoglobulin-like receptors strengthen CD8 + T cell–mediated control of HIV-1, HCV, and HTLV-1. Sci. Immunol. 3, 2892. 10.1126/sciimmunol.aao2892.

25. Khakoo SI, Thio CL, Martin MP, Brooks CR, Gao X, Astemborski J, Cheng J, Goedert JJ, Vlahov D, Hilgartner M, et al. (2004). HLA and NK cell inhibitory receptor genes in resolving hepatitis C virus infection. Science 305, 872–874. 10.1126/SCIENCE.1097670/SUPPL_FILE/KHAKOO_SOM.PDF. [PubMed: 15297676]

26. Martin MP, Gao X, Lee JH, Nelson GW, Detels R, Goedert JJ, Buchbinder S, Hoots K, Vlahov D, Trowsdale J, et al. (2002). Epistatic interaction between KIR3DS1 and HLA-B delays the progression to AIDS. Nat. Genet. 31, 429–434. 10.1038/NG934. [PubMed: 12134147]

27. Martin MP, Naranbhai V, Shea PR, Qi Y, Ramsuran V, Vince N, Gao X, Thomas R, Brumme ZL, Carlson JM, et al. (2018). Killer cell immunoglobulin–like receptor 3DL1 variation modifies HLA-B*57 protection against HIV-1. J. Clin. Invest. 128, 1903–1912. 10.1172/JCI98463. [PubMed: 29461980]

28. Ahlenstiel G, Martin MP, Gao X, Carrington M, and Rehermann B (2008). Distinct KIR/HLA compound genotypes affect the kinetics of human antiviral natural killer cell responses. J. Clin. Invest. 118, 1017–1026. 10.1172/JCI32400. [PubMed: 18246204]

29. Zhou X, Lee JE, Arnett FC, Xiong M, Park MY, Yoo YK, Shin ES, Reveille JD, Mayes MD, Kim JH, et al. (2009). HLA–DPB1 and DPB2 Are Genetic Loci for Systemic Sclerosis: A genome-wide association study in Koreans with replication in North Americans. Arthritis Rheum. 60, 3807–3814. 10.1002/art.24982. [PubMed: 19950302]

30. Wang J, Guo X, Yi L, Guo G, Tu W, Wu W, Yang L, Xiao R, Li Y, Chu H, et al. (2014). Association of HLA-DPB1 with Scleroderma and Its Clinical Features in Chinese Population. PLoS One 9, e87363. 10.1371/journal.pone.0087363. [PubMed: 24498086]

31. Al-Hussein KA, Rama NR, Ahmad M, Rozemuller E, and Tilanus MG (2003). HLA-DPB1*0401 is associated with dominant protection against type 1 diabetes in the general Saudi population and in subjects with a high-risk DR/DQ haplotype. Eur. J. Immunogenet. 30, 115–119. 10.1046/j.1365-2370.2003.00369.x. [PubMed: 12648278]

32. Varney MD, Valdes AM, Carlson JA, Noble JA, Tait BD, Bonella P, Lavant E, Fear AL, Louey A, Moonsamy P, et al. (2010). HLA DPA1, DPB1 Alleles and Haplotypes Contribute to the Risk Associated With Type 1 Diabetes. Diabetes 59, 2055–2062. 10.2337/db09-0680. [PubMed: 20424227]

33. Yamazaki T, Umemura T, Joshita S, Yoshizawa K, Tanaka E, and Ota M (2018). A cis-eQTL of HLA-DPB1 Affects Susceptibility to Type 1 Autoimmune Hepatitis. Sci. Rep. 8, 11924. 10.1038/S41598-018-30406-9. [PubMed: 30093645]

34. Niehrs A, Garcia-Beltran WF, Norman PJ, Watson GM, Hölzemer A, Chapel A, Richert L, Pommerening-Röser A, Körner C, Ozawa M, et al. (2019). A subset of HLA-DP molecules serve as ligands for the natural cytotoxicity receptor NKp44. Nat. Immunol. 20, 1129–1137. 10.1038/s41590-019-0448-4. [PubMed: 31358998]

35. Ting JP-Y, and Trowsdale J (2002). Genetic Control of MHC Class II Expression. Cell 109, S21–S33. 10.1016/S0092-8674(02)00696-7. [PubMed: 11983150]

36. Sallusto F, Lenig D, Förster R, Lipp M, and Lanzavecchia A (1999). Two subsets of memory T lymphocytes with distinct homing potentials and effector functions. Nature 401, 708–712. 10.1038/44385. [PubMed: 10537110]

37. Remmerswaal EBM, Hombrink P, Nota B, Pircher H, Ten Berge IJM, van Lier RAW, and van Aalderen MC (2019). Expression of IL-7Rα and KLRG1 defines functionally distinct CD8 +

T-cell populations in humans. Eur. J. Immunol. 49, 694–708. 10.1002/eji.201847897. [PubMed: 30883723]

38. Schreurs RRCE, Sagebiel AF, Steinert FL, Highton AJ, Klarenbeek PL, Drewniak A, Bakx R, The SML, Ribeiro CMS, Perez D, et al. (2021). Intestinal CD8+ T cell responses are abundantly induced early in human development but show impaired cytotoxic effector capacities. Mucosal Immunol. 14, 605–614. 10.1038/S41385-021-00382-X. [PubMed: 33772147]
39. van Leeuwen EMM, de Bree GJ, Remmerswaal EBM, Yong S-L, Tesselaar K, ten Berge IJM, and van Lier RAW (2005). IL-7 receptor a chain expression distinguishes functional subsets of virus-specific human CD8+ T cells. Blood 106, 2091–2098. 10.1182/blood-2005-02-0449. [PubMed: 15947093]
40. Klenerman P, and Oxenius A (2016). T cell responses to cytomegalovirus. Nat. Rev. Immunol. 16, 367–377. 10.1038/nri.2016.38. [PubMed: 27108521]
41. Al-Daccak R, Wang FQ, Theophille D, Lethielleux P, Colombani J, and Loiseau P (1991). Gene polymorphism of HLA-DPB1 and DPA1 loci in caucasoid population: Frequencies and DPB1-DPA1 associations. Hum. Immunol. 31, 277–285. 10.1016/0198-8859(91)90100-N. [PubMed: 1680839]
42. Alter G, Malenfant JM, and Altfeld M (2004). CD107a as a functional marker for the identification of natural killer cell activity. J. Immunol. Methods 294, 15–22. 10.1016/J.JIM.2004.08.008. [PubMed: 15604012]
43. Collier JL, Weiss SA, Pauken KE, Sen DR, and Sharpe AH (2021). Not-so-opposite ends of the spectrum: CD8+ T cell dysfunction across chronic infection, cancer and autoimmunity. Nat. Immunol, 809–819. 10.1038/s41590-021-00949-7. [PubMed: 34140679]
44. Pichler WJ, and Wyss-Coray T (1994). T cells as antigen-presenting cells. Immunol. Today Off. 15, 312–315. 10.1016/0167-5699(94)90078-7.
45. Hudrisier D, Riond J, Mazarguil H, Gairin JE, and Joly E (2001). Cutting Edge: CTLs Rapidly Capture Membrane Fragments from Target Cells in a TCR Signaling-Dependent Manner. J. Immunol. 166, 3645–3649. 10.4049/JIMMUNOL.166.6.3645. [PubMed: 11238601]
46. van Lier RAW, ten Berge IJM, and Gamadia LE (2003). Human CD8+ T-cell differentiation in response to viruses. Nat. Rev. Immunol. 3, 931–939. 10.1038/nri1254. [PubMed: 14647475]
47. Lau CM, Adams NM, Geary CD, Weizman O-E, Rapp M, Pritykin Y, Leslie CS, and Sun JC (2018). Epigenetic control of innate and adaptive immune memory. Nat. Immunol. 19, 963–972. 10.1038/s41590-018-0176-1. [PubMed: 30082830]
48. Gumá M, Angulo A, Vilches C, Gómez-Lozano N, Malats N, and López-Botet M (2004). Imprint of human cytomegalovirus infection on the NK cell receptor repertoire. Blood 104, 3664–3671. 10.1182/BLOOD-2004-05-2058. [PubMed: 15304389]
49. Schlums H, Cichocki F, Tesi B, Theorell J, Beziat V, Holmes TD, Han H, Chiang SCC, Foley B, Mattsson K, et al. (2015). Cytomegalovirus Infection Drives Adaptive Epigenetic Diversification of NK Cells with Altered Signaling and Effector Function. Immunity 42, 443–456. 10.1016/j.immuni.2015.02.008. [PubMed: 25786176]
50. Gumá M, Budt M, Sáez A, Brckalo T, Hengel H, Angulo A, and López-Botet M (2006). Expansion of CD94/NKG2C+ NK cells in response to human cytomegalovirus-infected fibroblasts. Blood 107, 3624–3631. 10.1182/blood2005-09-3682. [PubMed: 16384928]
51. van den Berg SPH, Pardieck IN, Lanfermeijer J, Sauce D, Klenerman P, van Baarle D, and Arens R (2019). The hallmarks of CMV-specific CD8 T-cell differentiation. Med. Microbiol. Immunol. 208, 365–373. 10.1007/s00430-019-00608-7. [PubMed: 30989333]
52. Lang PA, Crome SQ, Xu HC, Lang KS, Chapatte L, Deenick EK, Grusdat M, Pandyra AA, Pozdeev VI, Wang R, et al. (2020). NK Cells Regulate CD8+ T Cell Mediated Autoimmunity. Front. Cell. Infect. Microbiol. 10, 36. 10.3389/fcimb.2020.00036. [PubMed: 32117809]
53. Pallmer K, Barnstorf I, Baumann NS, Borsa M, Jonjic S, and Oxenius A (2019). NK cells negatively regulate CD8 T cells via natural cytotoxicity receptor (NCR) 1 during LCMV infection. PLoS Pathog. 15, e1007725. 10.1371/JOURNAL.PPAT.1007725. [PubMed: 30995287]
54. Zecher BF, Ellinghaus D, Schloer S, Niehrs A, Padoan B, Baumdick ME, Yuki Y, Martin MP, Glow D, Schröder-Schwarz J, et al. (2024). *HLA-DPA1*02:01~B1*01:01* is a risk haplotype

for primary sclerosing cholangitis mediating activation of NKp44+ NK cells. Gut 73, 325–337. 10.1136/gutjnl-2023-329524. [PubMed: 37788895]

55. Baumdick ME, Niehrs A, Degenhardt F, Schwerk M, Hinrichs O, Jordan-Paiz A, Padoan B, Wegner LHM, Schloer S, Zecher BF, et al. (2023). HLA-DP on Epithelial Cells Enables Tissue Damage by NKp44+ Natural Killer Cells in Ulcerative Colitis. Gastroenterology 165, 946–962.e13. 10.1053/j.gastro.2023.06.034. [PubMed: 37454979]
56. Yamazaki T, Umemura T, Joshita S, Yoshizawa K, Tanaka E, and Ota M (2018). A cis-eQTL of HLA-DPB1 Affects Susceptibility to Type 1 Autoimmune Hepatitis. Sci. Rep. 8, 11924. 10.1038/s41598-018-30406-9. [PubMed: 30093645]
57. Walter U, and Santamaria P (2005). CD8+ T cells in autoimmunity. Curr. Opin. Immunol. 17, 624–631. 10.1016/j.coi.2005.09.014. [PubMed: 16226438]
58. Petersdorf EW, Malkki M, O'hUigin C, Carrington M, Gooley T, Haagenson MD, Horowitz MM, Spellman SR, Wang T, and Stevenson P (2015). High HLA-DP Expression and Graft-versus-Host Disease. N. Engl. J. Med. 373, 599–609. 10.1056/NEJMOA1500140/SUPPL_FILE/NEJMOA1500140_DISCLOSURES.PDF. [PubMed: 26267621]
59. Pak CY, Eun HM, McArthur RG, and Yoon JW (1988). Association of Cytomegalovirus Infection With Autoimmune Type 1 Diabetes. Lancet 2, 1–4. 10.1016/S0140-6736(88)92941-8. [PubMed: 2898620]
60. Crispe IN, Dao T, Klugewitz K, Mehal WZ, and Metz DP (2000). The liver as a site of T-cell apoptosis: Graveyard, or killing field? Immunol. Rev. 174, 47–62. 10.1034/j.1600-0528.2002.017412.x. [PubMed: 10807506]
61. Poch T, Krause J, Casar C, Liwinski T, Glau L, Kaufmann M, Ahrenstorf AE, Hess LU, Ziegler AE, Martrus G, et al. (2021). Single-cell atlas of hepatic T cells reveals expansion of liver-resident naive-like CD4+ T cells in primary sclerosing cholangitis. J. Hepatol. 75, 414–423. 10.1016/J.JHEP.2021.03.016. [PubMed: 33774059]
62. Stuart T, Butler A, Hoffman P, Hafemeister C, Papalexi E, Mauck WM, Hao Y, Stoeckius M, Smibert P, and Satija R (2019). Comprehensive Integration of Single-Cell Data. Cell 177, 1888–1902.e21. 10.1016/J.CELL.2019.05.031. [PubMed: 31178118]
63. Wolock SL, Lopez R, and Klein AM (2019). Scrublet: Computational Identification of Cell Doublets in Single-Cell Transcriptomic Data. Cell Syst. 8, 281–291.e9. 10.1016/J.CELS.2018.11.005. [PubMed: 30954476]
64. Squair JW, Gautier M, Kathe C, Anderson MA, James ND, Hutson TH, Hudelle R, Qaiser T, Matson KJE, Barraud Q, et al. (2021). Confronting false discoveries in single-cell differential expression. Nat. Commun. 12, 5692–5715. 10.1038/s41467-021-25960-2. [PubMed: 34584091]
65. Yamashita Y, Anczurowski M, Nakatsugawa M, Tanaka M, Kagoya Y, Sinha A, Chamoto K, Ochi T, Guo T, Saso K, et al. (2017). HLA-DP84Gly constitutively presents endogenous peptides generated by the class I antigen processing pathway. Nat. Commun, 15244–15314. 10.1038/ncomms15244. [PubMed: 28489076]
66. Schultheiß C, Paschold L, Simnica D, Mohme M, Willscher E, von Wenserski L, Scholz R, Wieters I, Dahlke C, Tolosa E, et al. (2020). Next-Generation Sequencing of T and B Cell Receptor Repertoires from COVID-19 Patients Showed Signatures Associated with Severity of Disease. Immunity 53, 442–455.e4. 10.1016/J.IMMUNI.2020.06.024. [PubMed: 32668194]
67. Schultheiß C, Simnica D, Willscher E, Oberle A, Fanchi L, Bonzanni N, Wildner NH, Schulze Zur Wiesch J, Weiler-Normann C, Lohse AW, and Binder M (2021). Next-Generation Immunosequencing Reveals Pathological T-Cell Architecture in Autoimmune Hepatitis. Hepatology 73, 1436–1448. 10.1002/HEP.31473. [PubMed: 32692457]
68. Brüggemann M, Kotrová M, Knecht H, Bartram J, Boudjogrha M, Bystry V, Fazio G, Froňková E, Giraud M, Grioni A, et al. (2019). Standardized next-generation sequencing of immunoglobulin and T-cell receptor gene recombinations for MRD marker identification in acute lymphoblastic leukaemia; a EuroClonality-NGS validation study. Leukemia 33, 2241–2253. 10.1038/s41375-019-0496-7. [PubMed: 31243313]
69. van Dongen JJM, Langerak AW, Brüggemann M, Evans PAS, Hummel M, Lavender FL, Delabesse E, Davi F, Schuuring E, García-Sanz R, et al. (2003). Design and standardization of PCR primers and protocols for detection of clonal immunoglobulin and T-cell receptor gene recombinations

in suspect lymphoproliferations: Report of the BIOMED-2 Concerted Action BMH4-CT98–3936. Leukemia, 2257–2317. 10.1038/sj.leu.2403202. [PubMed: 14671650]

70. Bolotin DA, Poslavsky S, Mitrophanov I, Shugay M, Mamedov IZ, Putintseva EV, and Chudakov DM (2015). MiXCR: software for comprehensive adaptive immunity profiling. Nat. Methods, 380–381. 10.1038/nmeth.3364. [PubMed: 25924071]
71. Simnica D, Schliffke S, Schultheiß C, Bonzanni N, Fanchi LF, Akyüz N, Gösch B, Casar C, Thiele B, Schlüter J, et al. (2019). High-throughput immunogenetics reveals a lack of physiological T cell clusters in patients with autoimmune cytopenias. Front. Immunol. 10, 473693. 10.3389/FIMMU.2019.01897/BIBTEX.
72. Simnica D, Akyüz N, Schliffke S, Mohme M, v.Wenserski L, Mährle T, Fanchi LF, Lamszus K, and Binder M (2019). T cell receptor next-generation sequencing reveals cancer-associated repertoire metrics and reconstitution after chemotherapy in patients with hematological and solid tumors. OncoImmunology 8, e1644110. 10.1080/2162402X.2019.1644110. [PubMed: 31646093]

Highlights

- Effector $CD8^+$ T cells express on their surface the HLA class II heterodimer HLA-DP
- Expression of HLA-DP on effector $CD8^+$ T cells is upregulated upon HCMV infection
- $NKp44^+$ NK cells interact with $CD8^+$ T cells carrying NKp44-binding HLA-DP molecules
- $CD8^+$ T cells expressing NKp44-binding HLA-DPs show reduced clonal expansion

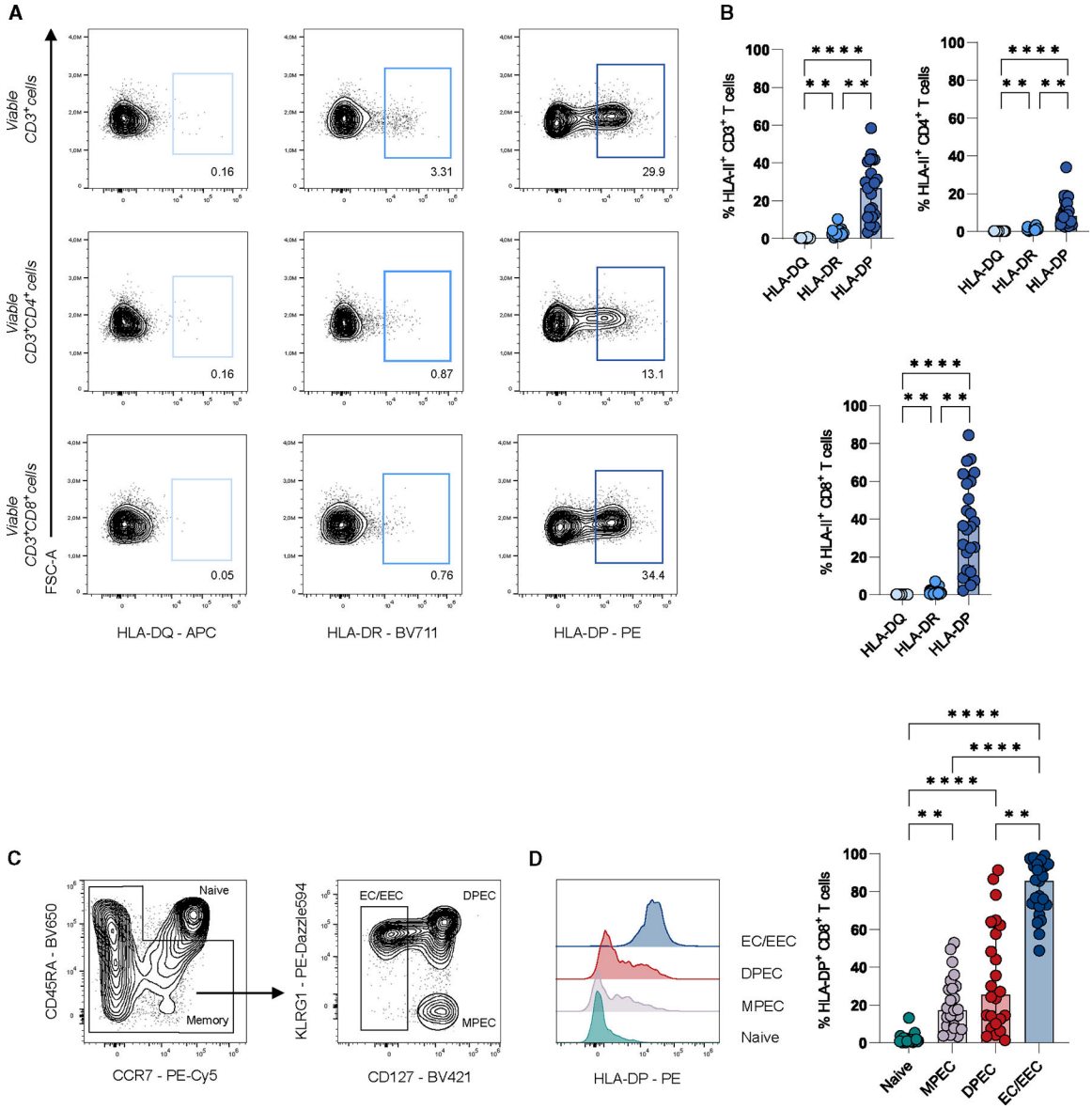

Figure 1. HLA-DP is expressed *ex vivo* on CD8$^+$ T cells

(A) Representative flow cytometric plots showing the applied gating strategy used to identify HLA-II molecules (HLA-DQ, HLA-DR, HLA-DP) in viable CD3$^+$, CD3$^+$ CD4$^+$, and CD3$^+$ CD8$^+$ T cells.

(B). Median percentage (± interquartile range [IQR]) of HLA-DQ, HLA-DR, and HLA-DP on T cells (CD3$^+$, CD3$^+$ CD4$^+$, and CD3$^+$ CD8$^+$ T cells). Shown are $n = 24$ samples, and each dot represents one biological replicate. Statistical significance was determined using the two-tailed Friedman test with post hoc Dunn's correction. $^{**}p = 0.0016$ and $^{****}p < 0.0001$.

(C) (Left) Representative flow cytometric plot of CD45RA and CCR7 expression on CD8$^+$ T cells used to define naive (CD45RA$^+$ CCR7$^+$) and memory T cells. (Right) The memory subset was further analyzed using KLRG1 and CD127 expression, defining MPEC (CD127$^+$

KLRG1^{-}), DPEC (CD127^{+} KLRG1^{+}), and EC/EEC (CD127^{-} KLRG1$^{-/+}$) CD8^{+} T cell populations.

(D) (Left) Representative histogram and (right) median percentage (±IQR) of HLA-DP expression on gated naive, MPEC, DPEC, and EC/EEC CD8^{+} T cells. Shown are n = 24 samples, and each dot represents one biological replicate. Statistical significance was determined using the two-tailed Friedman test with post hoc Dunn's correction. **p = 0.0071 and ****$p < 0.0001$.

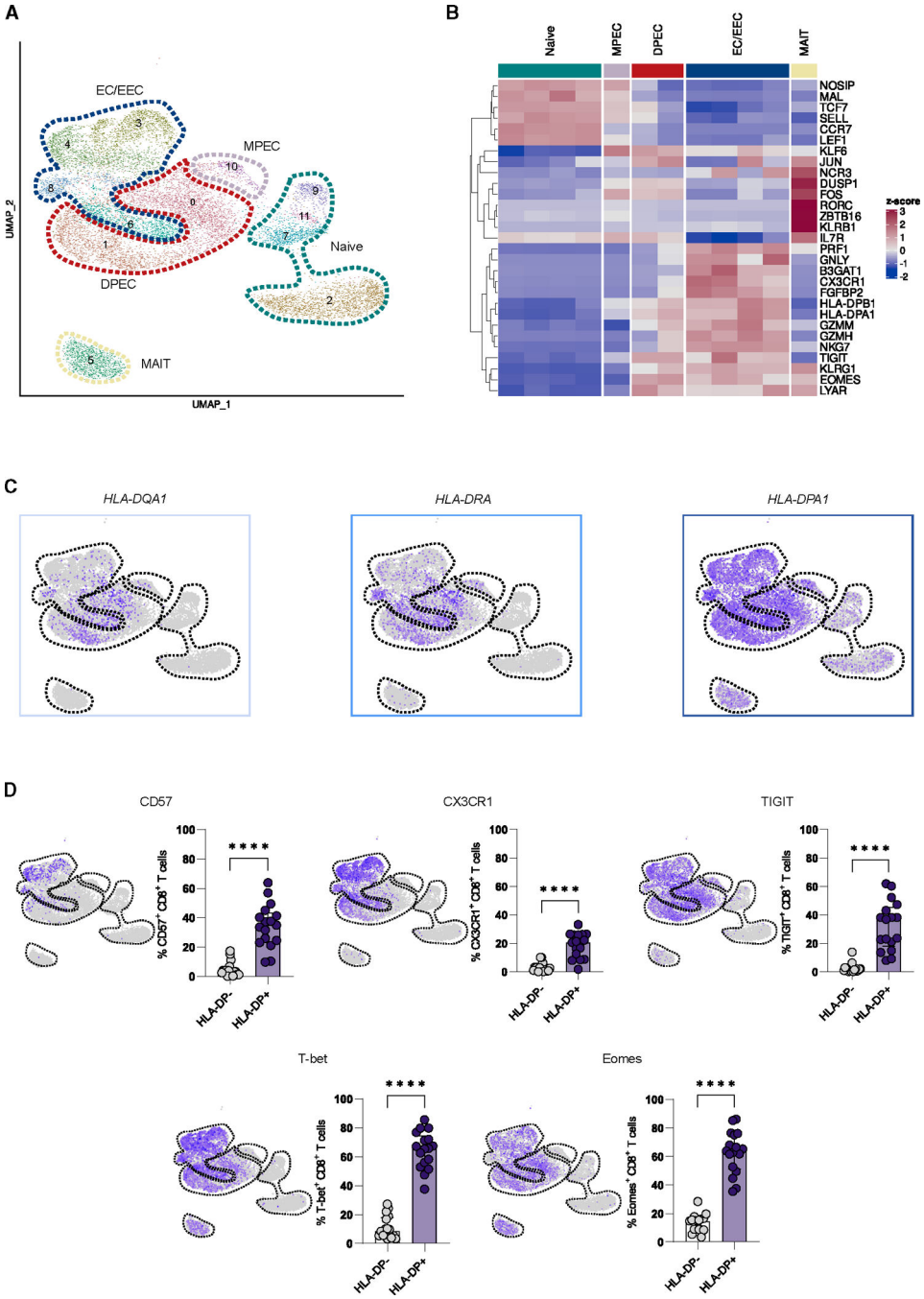

Figure 2. *HLA-DP* mRNA is transcribed in CD8$^+$ T cells

(A) Uniform manifold approximation and projection (UMAP) of merged scRNA-seq profiles of sorted CD8$^+$ T cells. The different clusters are grouped in subsets based on manual annotation. Two subsets were too sparse for analysis and were excluded (12–13). n = 12.946 cells are plotted from n = 3 combined samples.

(B) Cluster heatmap highlighting differentially expressed genes (DEGs) signatures for manually annotated subsets.

(C) UMAP representation of HLA-II α-chain transcript average expression (*HLA-DQA1, HLA-DRA, HLA-DPA1*).

(D) UMAP representation (left) and representative flow cytometric plot (right) of median percentage (±IQR) of CD57, CX3CR1, TIGIT, T-bet, and Eomes. Shown are $n = 17$ samples, and each dot represents one biological replicate. Statistical significance was determined using two-tailed Wilcoxon matched-pairs signed-rank test. ****$p < 0.0001$.

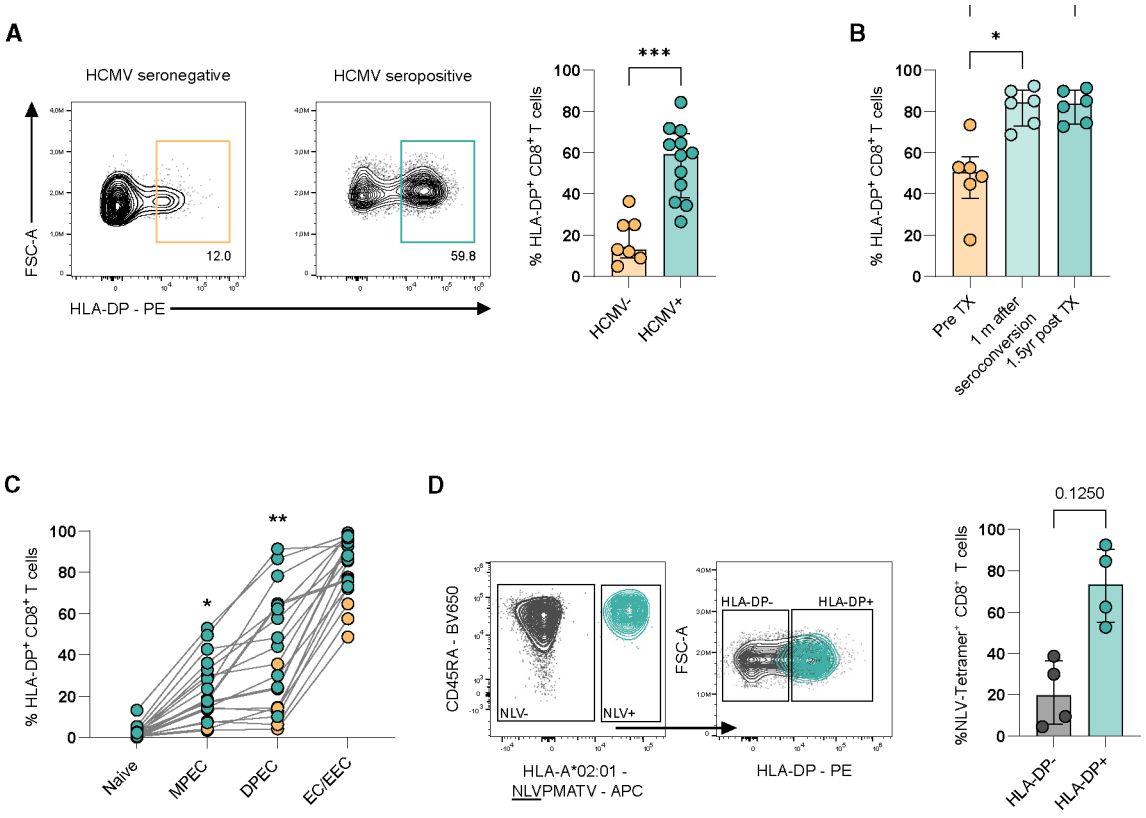

Figure 3. HLA-DP is upregulated in HCMV-seropositive individuals

(A) (Left) Representative flow cytometric plots showing the applied gating strategy; (right) median percentage (±IQR) of HLA-DP$^+$ CD8$^+$ T cells from HCMV-seronegative and -seropositive individuals. Shown are $n = 19$ different samples (HCMV^{neg} = 7; HCMV^{pos} = 12), and each dot represents one biological replicate. Statistical significance was determined using Mann-Whitney test. ***$p = 0.0003$.

(B) Median percentage (±IQR) of HLA-DP$^+$ CD8$^+$ T cells. Shown are $n = 6$ different samples from three different time points. One sample from Pre TX was collected 1 week post-transplantation (TX). Statistical significance was determined using two-tailed Friedman test with post hoc Dunn's correction. *$p = 0.03$.

(C) Percentage of HLA-DP$^+$ CD8$^+$ T cells within gated naive, MPEC, DPEC, and EC/EEC CD8$^+$ T cells from HCMV-seronegative and -seropositive individuals. Shown are $n = 19$ different samples (HCMV^{neg} = 7; HCMV^{pos} = 12), and each dot represents one biological replicate. Gray lines connect the same biological replicate. Statistical significance was determined using Mann-Whitney test. *$p = 0.01$ and **$p = 0.002$. See also Figure S3A.

(D) (Left) Representative flow cytometric plot showing the applied gating strategy used to identify HLA-A*02:01-NLVPMVATV tetramer$^{-/+}$ CD8$^+$ T cells. Only individuals with >150 events within the NLV$^+$ gate were considered for subsequent analysis. (Middle) Representative flow cytometric plot showing the applied gating strategy used to identify HLA-DP$^{-/+}$ HLA-A*02:01–NLVPMVATV tetramer$^+$ CD8$^+$ T cells. (Right) Median percentage (±IQR) of HLA-DP$^-$ and HLA-DP$^+$ HLA-A*02:01-NLVPMVATV tetramer$^+$ CD8$^+$ T cells. Shown are results from $n = 4$ individuals, and each dot represents one

biological replicate. Statistical significance was determined using Wilcoxon matched-pairs signed-rank test.

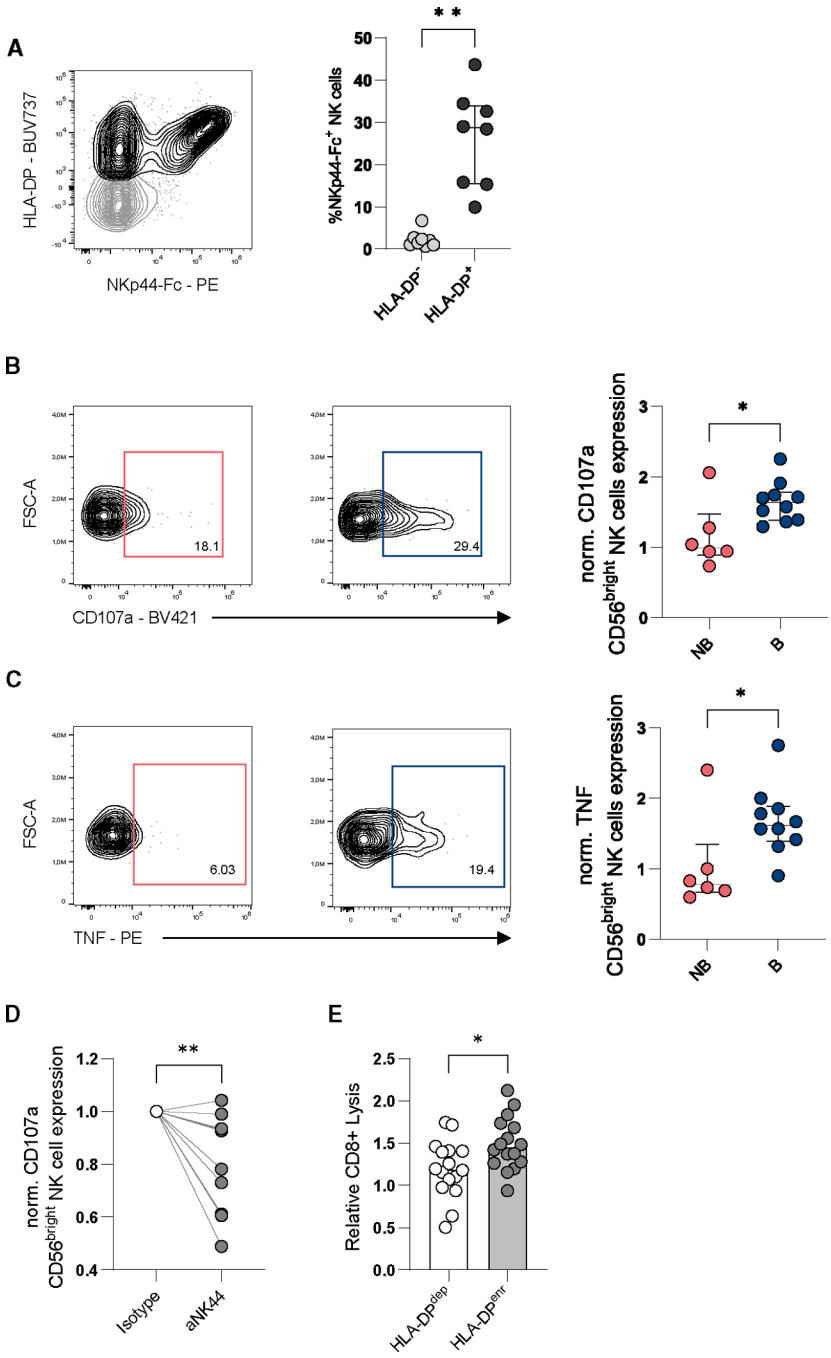

Figure 4. NKp44 binds HLA-DP$^+$ CD8$^+$ T cells in a haplotype-dependent process

(A) (Left) Representative flow cytometric plot showing NKp44-Fc construct binding to HLA-DP$^{-/+}$ CD8$^+$ T cells. (Right) Median percentage (±IQR) of NKp44-Fc binding to CD8$^+$ HLA-DP$^{-/+}$ T cells. Dots represent four donors in technical duplicates (n = 8). Statistical significance was determined using Wilcoxon matched-pairs signed-rank test. **p = 0.008.

(B) (Left) Representative flow cytometric plots showing the applied gating strategy used to identify CD107a$^+$ CD56^{bright} NK cells after co-incubation with autologous CD8$^+$ T cells

from individuals with NKp44 non-binding (NB) and -binding (B) HLA-DP antigens. (Right) Median (±IQR) of normalized CD107a expression of $CD56^{bright}$ NK cells based on negative control NK cells only. NB dots represent three technical replicates from 2 individuals (n = 6). B dots represent three technical replicates from 3 individuals and one replicate from one individual (n = 10). Statistical significance was determined using Mann-Whitney test. *p = 0.02.

(C) (Left) Representative flow cytometric plots showing the applied gating strategy to identify TNF^+ $CD56^{bright}$ NK cells after co-incubation with autologous $CD8^+$ T cells from individuals with NKp44 NB and -B HLA-DP antigens. (Right) Median (±IQR) of normalized TNF expression of $CD56^{bright}$ NK cells based on negative control NK cells only. NB dots represent three technical replicates from 2 individuals (n = 6). B dots represent three technical replicates from 3 individuals and one replicate from one individual (n = 10). Statistical significance was determined using Mann-Whitney test. *p = 0.03.

(D) Plot shows fold change in degranulation (CD107a expression) of $CD56^{bright}$ NK cells after coincubation with autologous $CD8^+$ T cells from individuals with NKp44-B HLA-DP antigens in the presence of an isotype or anti-NKp44 blocking antibody. Dots represent 4 donors (one of them twice) in technical duplicates (n = 10). Statistical significance was determined using Wilcoxon matched-pairs signed-rank test. **p = 0.006.

(E) Plot shows the median of NK cell-mediated cytotoxicity after co-incubation with autologous $CD8^+$ T cells from individuals with NKp44-B HLA-DP antigens. Data are presented as relative $CD8^+$ T cell lysis calculated by dividing the lactate dehydrogenase (LDH) release of NK cell and $CD8^+$ T cell cocultures with spontaneous LDH release of $CD8^+$ T cells cultured alone without NK cells. Dots represent data from 4 donors in technical quadruplicates from the same experiment (n = 16). Statistical significance was determined using Wilcoxon matched-pairs signed-rank test. *p = 0.02.

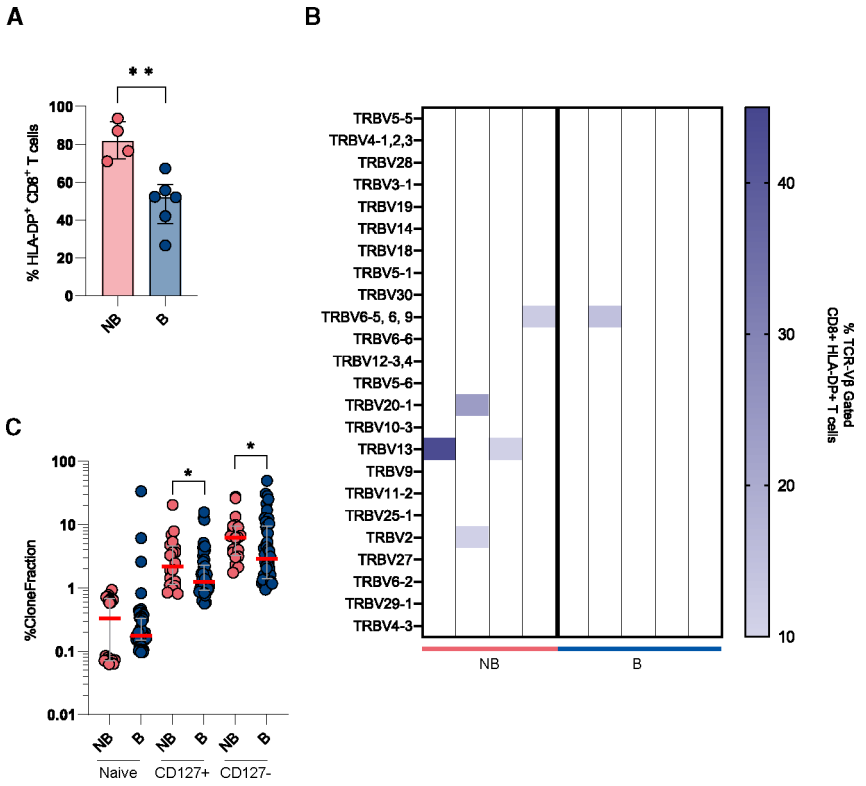

Figure 5. CD8$^+$ T cells hyper-expand in individuals with HLA-DP haplotypes not recognized by NKp44

(A) Median percentage (±IQR) of HLA-DP$^+$ CD8$^+$ T cells from individuals with two NKp44-NB (n = 4) compared to two NKp44-B (n = 6) HLA-DP haplotypes. Statistical significance was determined using Mann-Whitney test. **p = 0.0095. Each dot represents one biological replicate.

(B) Heatmap displaying percentages of CD8$^+$ HLA-DP$^+$ T cells with hyper-expanded TCR Vβ chains from individuals with two NKp44 NB (n = 4) compared to two NKp44-B (n = 5) HLA-DP haplotypes. Threshold for hyper-expansion = 10%. Statistical significance was determined using Fisher's exact test. *p = 0.0476 (n = 9). Each line divides one biological replicate.

(C) Median (±IQR) of clone fraction percentage of the top 10 expanded clones from CD8$^+$ naive, CD127$^+$, and CD127$^-$ T cells of individuals with two NKp44 NB (n = 2) compared to two NKp44-B (n = 5) HLA-DP haplotypes. Statistical significance was determined using Mann-Whitney test. CD127$^+$ *p = 0.0296; CD127$^-$ *p = 0.0421.

Table 1.

HLA-DP-NKp44 non-binding and binding

Individual	Haplotype 1	Binding	Haplotype 2	Binding
1	DPA1*01:03~DPB1*03:01	NB	DPA1*02:01~DPB1*14:01	NB
2	DPA1*01:03~DPB1*03:01	NB	DPA1*02:01~DPB1*14:01	NB
3	DPA1*01:03~DPB1*03:01	NB	DPA1*01:03~DPB1*03:01	NB
4	DPA1*02:02~DPB1*05:01	NB	DPA1*02:02~DPB1*05:01	NB
5	DPA1*01:03~DPB1*04:01	B	DPA1*01:03~DPB1*04:01	B
6	DPA1*01:03~DPB1*04:01	B	DPA1*01:03~DPB1*04:01	B
7	DPA1*01:03~DPB1*02:01	B	DPA1*01:03~DPB1*04:01	B
8	DPA1*01:03~DPB1*04:01	B	DPA1*01:03~DPB1*04:01	B
9	DPA1*01:03~DPB1*04:01	B	DPA1*01:03~DPB1*04:01	B

HLA-DP antigens were defined as HLA-DP-NKp44 non-binding (NB) and HLA-DP-NKp44 binding (B) accordingly to Niehrs et al.[34]

KEY RESOURCES TABLE

REAGENT or RESOURCE	SOURCE	IDENTIFIER
Antibodies		
CD3 – BUV395 (UCHT-1)	BD Biosciences	Cat#563546; RRID:AB_2744387
CD3 – BUV496 (UCHT-1)	BD Biosciences	Cat# 612940; RRID:AB_2870222
CD127 – BV421 (A019D5)	BioLegend	Cat#351310; RRID:AB_10960140
CD19 – BV510 (HIB19)	BioLegend	Cat#302242; RRID:AB_2561668
CD4 – BV570 (RPA-T4)	BioLegend	Cat#300534; RRID:AB_2563791
CD4 – BV711 (RPA-T4)	BioLegend	Cat# 300558; RRID:AB_2564393
CD4 – BUV747 (SK3)	BD Biosciences	Cat# 612748; RRID:AB_2870079
CD45RA – BV650 (HI100)	BD Biosciences	Cat#563963; RRID:AB_2738514
HLA-DR – BV711 (L243)	BioLegend	Cat#307644; RRID:AB_2562913
CD8 – BV785 (RPA-T8)	BioLegend	Cat#301046; RRID:AB_2563264
CD8 – FITC (RPA-T8)	BioLegend	Cat# 301006; RRID:AB_314124
CD8 – FITC (SK1)	BioLegend	Cat# 344704; RRID:AB_1877178
CD27 – FITC (O323)	BioLegend	Cat#302806; RRID:AB_314298
CD27 – BV605 (O323)	BioLegend	Cat# 302830; RRID:AB_2561450
CX3CR1 – PerCP-Cy5.5 (2a9-1)	BioLegend	Cat#341614; RRID:AB_11219203
CX3CR1 – PE/Cyanine7 (2A9-1)	BioLegend	Cat# 341612; RRID:AB_10900816
HLA-DP – PE (B7/21)	BD Biosciences	Cat#566825; RRID:AB_2869887
HLA-DP – BUV737 (B7/21)	BD Biosciences	Cat# 750942; RRID:AB_2875023
KLRG1 – PE-Dazzle594 (SA231A2)	BioLegend	Cat#367710; RRID:AB_2572155
CCR7 – PE/Cyanine5 (G043H7)	BioLegend	Cat# 353271; RRID:AB_2904373
HLA-DQ – APC (1a3)	Leinco Technologies	Cat# H242; RRID:AB_2893760
CD14 – Alexa Fluor 700 (63D3)	BioLegend	Cat# 367114; RRID:AB_2566716
CD14 – Alexa Fluor 700 (M5E2)	BioLegend	Cat# 301822; RRID:AB_493747
CD20 – Alexa Fluor 700 (2H7)	BioLegend	Cat# 302322; RRID:AB_493753
CD57 – BV510 (QA17A04)	BioLegend	Cat# 393314; RRID:AB_2750342
CD56 – BV605 (HCD56)	BioLegend	Cat# 318334; RRID:AB_2561912
CD16 – PerCP-Cy5.5 (3G8)	BioLegend	Cat# 302027; RRID:AB_893263
CD16 – FITC (3G8)	BioLegend	Cat# 302006; RRID:AB_314206
CD107a – BV421 (H4A3)	BioLegend	Cat# 328626; RRID:AB_11203537
TNF-α – PE (MAb11)	BioLegend	Cat# 502909; RRID:AB_315261
NKp44 – Alexa Fluor 647 (P44-8)	BioLegend	Cat# 325112; RRID:AB_2149431
TIGIT – BV605 (A15153G)	BioLegend	Cat# 372712; RRID:AB_2632927
T-bet – BV711 (4B10)	BioLegend	Cat# 644820; RRID:AB_2715766
EOMES Monoclonal Antibody – PerCP-eFluor™ 710 (WD1928), eBioscience	Thermo Fisher Scientific	Cat# 46-4877-42; RRID:AB_2573759
F(ab')2-Goat anti-Human IgG Fc Secondary Antibody – PE	Thermo Fisher Scientific	Cat# H10104; RRID:AB_2536546
Ultra-LEAF™ Purified Mouse IgG1, κ Isotype Ctrl Antibody	BioLegend	Cat#400166; RRID:AB_2927801
Ultra-LEAF(TM) Purified anti-human CD336 (NKp44)	BioLegend	Cat#325122; RRID:AB_2819954
TotalSeq™-A0048 Anti-Human CD45 (2D1)	BioLegend	Cat# 368543; RRID:AB_2734418

REAGENT or RESOURCE	SOURCE	IDENTIFIER
TotalSeq™-A0063 anti-human CD45RA	BioLegend	Cat# 304157; RRID:AB_2734267
TotalSeq™-A0148 anti-human CCR7	BioLegend	Cat# 353247; RRID:AB_2750357
Purified Anti-Human CD45 (2D1)	BioLegend	Cat# 368502; RRID:AB_2566240
Biological samples		
Human blood	Healthy Hamburg cohort	N/A
Human PBMCs	Academic Medical Center, Amsterdam	N/A
Chemicals, peptides, and recombinant proteins		
Recombinant Human NKp44 Fc Chimera Protein, CF	R&D Systems	Cat#2249-NK-050
B2M Peptide: FYLLYYTEFTPT	GenScript Biotech	N/A
HLA-A*02:01 NLVPMVATC – APC	Tetramer Shop	Cat#HLA02-010
Lymphocyte Separation Medium, Density 1.077 g/mL	Capricorn Scientific	Cat#LSM-A
Fetal Bovine Serum Advanced (FBS Advanced)	Capricorn Scientific	Cat#FBS-11A
Dymethyl sulfoxide (DMSO)	Sigma-Aldrich	Cat#D5879-100ML
Dulbecco's phosphate buffered saline (PBS)	Sigma-Aldrich	Cat#D8537
Paraformaldehyde	Sigma-Aldrich	Cat#P6148
BD Cytofix/Cytoperm Fixation and Permeabilization Solution	BD Biosciences	Cat#554722
eBioscience™ Foxp3/Transcription Factor Staining Buffer Set	Invitrogen™	Cat#00-5523-00
autoMACS Running Buffer	Miltenyi Biotec	Cat#130-091-221
Recombinant Human IL-2	PeproTech	Cat#200-02
Recombinant Human IL-15	PeproTech	Cat#200-15
Gibco™ RPMI 1640 Medium	Thermo Fisher Scientific	Cat#12004997
Brefeldin A	Sigma-Aldrich	Cat#B7651-5MG
Critical commercial assays		
LIVE/DEAD™ Fixable Near-IR Dead Cell Stain Kit, for 633 or 635 nm excitation	Invitrogen™	Cat#L34976
10x V3 B Chip GEM generation kit	10x Genomics	N/A
Beta Mark TCR Vbeta Repertoire Kit, 25 Tests, RUO	Beckman Coulter	Cat#IM3497
Human Anti-Cytomegalovirus IgG ELISA Kit (CMV)	Abcam	Cat#ab108724
EasySep™ Human $CD8^+$ T cell Enrichment Kit	StemCell Technologies	Cat#19053
EasySep™ Human NKCell Enrichment Kit	StemCell Technologies	Cat#19055
Anti-PE MicroBeads	Miltenyi Biotec	Cat#130-048-801
MS Columns	Miltenyi Biotec	Cat#130-042-201
OctoMACS™ Separator	Miltenyi Biotec	Cat#130-042-109
CyQUANT™ LDH Cytotoxicity Assay	Invitrogen	Cat#C20300
Deposited data		
RNAseq - Figure 2	This paper	Array Express: E-MTAB-13405
TCR – Figure 5C	This paper	ENA: PRJEB66421

REAGENT or RESOURCE	SOURCE	IDENTIFIER
Software and algorithms		
Magellan software version 6.1	TECAN	https://lifesciences.tecan.com/software-magellan
FlowJo 10.8 software	BD Biosciences	https://www.flowjo.com/
CellRanger	10x Genomics	https://support.10xgenomics.com/
R Studio	R Project	https://www.r-project.org/